REPORT DOCUMENTATION PAGE

Form Approved
OMB No. 0704-0188

PLEASE DO NOT RETURN YOUR FORM TO THE ABOVE ORGANIZATION.

1. REPORT DATE *(DD-MM-YYYY)*	2. REPORT TYPE	3. DATES COVERED *(From - To)*
29-07-2013	Final	Nov 2009-Oct 2012

4. TITLE AND SUBTITLE

Thermosphere Density Variability, Drag Coefficients, and Precision Satellite Orbits

5a. CONTRACT NUMBER

5b. GRANT NUMBER

FA9550-10-1-0038

5c. PROGRAM ELEMENT NUMBER

6. AUTHOR(S)

McLaughlin, Craig A.; Mysore Krishna, Dhaval; Mehta, Piyush M.; Lechtenberg, Travis F.; Hiatt, Andrew; Fattig, Eric; and Locke, Travis

5d. PROJECT NUMBER

5e. TASK NUMBER

5f. WORK UNIT NUMBER

7. PERFORMING ORGANIZATION NAME(S) AND ADDRESS(ES)

University of Kansas, Aerospace Engineering
1530 W. 15th St
Lawrence, KS 66045

8. PERFORMING ORGANIZATION REPORT NUMBER

9. SPONSORING/MONITORING AGENCY NAME(S) AND ADDRESS(ES)

AFOSR/RTB
875 N. Randolph St., Suite 3112
Arlington, VA 22203

10. SPONSOR/MONITOR'S ACRONYM(S)

AFOSR/RTB

11. SPONSOR/MONITOR'S REPORT NUMBER(S)

AFRL-OSR-VA-TR-2013-0428

12. DISTRIBUTION/AVAILABILITY STATEMENT

Approved for Public Release; Distribution is Unlimited.

13. SUPPLEMENTARY NOTES

14. ABSTRACT

This research used precision orbit data to estimate neutral density along the orbits of the CHAMP, GRACE, and TerraSAR-X orbits. Comparisons with accelerometer data showed the precision orbit derived densities were more accurate than densities from the High Accuracy Satellite Model or from commonly used empirical density models. Additional research showed that the high frequency variations in density observed only be accelerometers have little effect on orbit propagation accuracy. CHAMP and GRACE precision orbit data were decimated to 8 and 15 minutes per orbit and had noise levels up to 100 m added to them to observe the effects of limited data of lower accuracy on density estimation. As expected, the accuracy decreased as higher levels of noise were added to the data, but the even with limited data of moderate accuracy, the estimated densities were of usable accuracy. The Direct Simulation Monte Carlo was used to estimate drag coefficients for the GRACE, Stella, and Starlette satellites. The resulting drag coefficients showed good agreement with existing drag coefficient techniques.

15. SUBJECT TERMS

Satellite Drag; Thermosphere; Neutral Density; Precision Orbit Determination; Ballistic Coefficient; Drag Coefficient; DSMC

16. SECURITY CLASSIFICATION OF:			17. LIMITATION OF ABSTRACT	18. NUMBER OF PAGES	19a. NAME OF RESPONSIBLE PERSON
a. REPORT	b. ABSTRACT	c. THIS PAGE			Craig A. McLaughlin
U	U	U	U		19b. TELEPHONE NUMBER *(Include area code)* 785-864-2967

Reset

Standard Form 298 (Rev. 8/98)
Prescribed by ANSI Std. Z39.18

INSTRUCTIONS FOR COMPLETING SF 298

1. REPORT DATE. Full publication date, including day, month, if available. Must cite at least the year and be Year 2000 compliant, e.g. 30-06-1998; xx-06-1998; xx-xx-1998.

2. REPORT TYPE. State the type of report, such as final, technical, interim, memorandum, master's thesis, progress, quarterly, research, special, group study, etc.

3. DATES COVERED. Indicate the time during which the work was performed and the report was written, e.g., Jun 1997 - Jun 1998; 1-10 Jun 1996; May - Nov 1998; Nov 1998.

4. TITLE. Enter title and subtitle with volume number and part number, if applicable. On classified documents, enter the title classification in parentheses.

5a. CONTRACT NUMBER. Enter all contract numbers as they appear in the report, e.g. F33615-86-C-5169.

5b. GRANT NUMBER. Enter all grant numbers as they appear in the report, e.g. AFOSR-82-1234.

5c. PROGRAM ELEMENT NUMBER. Enter all program element numbers as they appear in the report, e.g. 61101A.

5d. PROJECT NUMBER. Enter all project numbers as they appear in the report, e.g. 1F665702D1257; ILIR.

5e. TASK NUMBER. Enter all task numbers as they appear in the report, e.g. 05; RF0330201; T4112.

5f. WORK UNIT NUMBER. Enter all work unit numbers as they appear in the report, e.g. 001; AFAPL30480105.

6. AUTHOR(S). Enter name(s) of person(s) responsible for writing the report, performing the research, or credited with the content of the report. The form of entry is the last name, first name, middle initial, and additional qualifiers separated by commas, e.g. Smith, Richard, J, Jr.

7. PERFORMING ORGANIZATION NAME(S) AND ADDRESS(ES). Self-explanatory.

8. PERFORMING ORGANIZATION REPORT NUMBER. Enter all unique alphanumeric report numbers assigned by the performing organization, e.g. BRL-1234; AFWL-TR-85-4017-Vol-21-PT-2.

9. SPONSORING/MONITORING AGENCY NAME(S) AND ADDRESS(ES). Enter the name and address of the organization(s) financially responsible for and monitoring the work.

10. SPONSOR/MONITOR'S ACRONYM(S). Enter, if available, e.g. BRL, ARDEC, NADC.

11. SPONSOR/MONITOR'S REPORT NUMBER(S). Enter report number as assigned by the sponsoring/ monitoring agency, if available, e.g. BRL-TR-829; -215.

12. DISTRIBUTION/AVAILABILITY STATEMENT. Use agency-mandated availability statements to indicate the public availability or distribution limitations of the report. If additional limitations/ restrictions or special markings are indicated, follow agency authorization procedures, e.g. RD/FRD, PROPIN, ITAR, etc. Include copyright information.

13. SUPPLEMENTARY NOTES. Enter information not included elsewhere such as: prepared in cooperation with; translation of; report supersedes; old edition number, etc.

14. ABSTRACT. A brief (approximately 200 words) factual summary of the most significant information.

15. SUBJECT TERMS. Key words or phrases identifying major concepts in the report.

16. SECURITY CLASSIFICATION. Enter security classification in accordance with security classification regulations, e.g. U, C, S, etc. If this form contains classified information, stamp classification level on the top and bottom of this page.

17. LIMITATION OF ABSTRACT. This block must be completed to assign a distribution limitation to the abstract. Enter UU (Unclassified Unlimited) or SAR (Same as Report). An entry in this block is necessary if the abstract is to be limited.

Thermosphere Density Variability, Drag Coefficients, and Precision Satellite Orbits

Craig A. McLaughlin, Dhaval Mysore Krishna, Piyush M. Mehta, Travis Lechtenberg, Andrew Hiatt, Eric Fattig, and Travis Locke

Abstract

Precision orbit ephemerides (POE) are used to estimate atmospheric density along the orbits of CHAMP (Challenging Minisatellite Payload) and GRACE (Gravity Recovery and Climate Experiment). The densities are calibrated against accelerometer derived densities and considering ballistic coefficient estimation results. The 14-hour density solutions are stitched together using a linear weighted blending technique to obtain continuous solutions over the entire mission life of CHAMP and through 2011 for GRACE. POE derived densities outperform the High Accuracy Satellite Drag Model (HASDM), NRLMSISE-00 model, and Jacchia 71 model densities when comparing cross correlation and RMS with accelerometer derived densities. Cross correlations for all other data sets with accelerometer derived densities are lower when the satellite's orbit planes are near the terminator. Additional research showed that the high frequency variations in density observed only be accelerometers have little effect on orbit propagation accuracy. CHAMP and GRACE precision orbit data were decimated to 8 and 15 minutes per orbit and had noise levels up to 100 m added to them to observe the effects of limited data of lower accuracy on density estimation. As expected, the accuracy decreased as higher levels of noise were added to the data, but the even with limited data of moderate accuracy, the estimated densities were of usable accuracy. The Direct Simulation Monte Carlo was used to estimate drag coefficients for the GRACE, Stella, and Starlette satellites. The resulting drag coefficients showed good agreement with existing drag coefficient techniques. The models were also used to develop a new empirical drag coefficient model for GRACE, which can be easily extended to other satellites. The empirical model allows computationally efficient determination of drag coefficients for complex satellites.

1 Introduction

Atmospheric density and drag coefficient modeling have long been among the greatest uncertainties in the ability to predict the motion of low Earth orbit (LEO) satellites, which is a critical aspect of space situational awareness (SSA). Accurate density and drag coefficient calculations are required to provide meaningful estimates of the atmospheric drag perturbing satellite motion. These effects increase with lower altitude orbits and also with higher effective area and lower mass satellites. The proposed effort will use precision satellite orbits to examine thermospheric density changes and examine techniques for improving satellite drag coefficient modeling.

The long term objectives of the PI are to improve capabilities in the area of SSA by improving orbit estimation and prediction for LEO satellites, better understanding the density fluctuations in the thermosphere, and improving the transfer of knowledge between the aeronomy and orbital mechanics communities. The specific objectives of this proposed effort were to:

1. Better understand the density variations in the thermosphere by using precision orbit ephemeris (POE) derived density data from several satellites to simultaneously examine the fluctuations in atmospheric density over time scales ranging from two hours to one day and correlate these fluctuations with specific upper atmospheric phenomena. How does atmospheric density change in both time and in space? How do these changes affect the motion of satellites? These are some of the fundamental questions that this research will address.

2. Better understand the relationship between drag coefficient models and orbit determination and prediction accuracy. This objective will examine the limitation of existing theories for satellite drag

coefficients. In addition, the research will examine whether modern computational fluids techniques are applicable to this problem and worth the increased computational burden they impose.

2 Density Estimation

2.1 Background

McLaughlin (2005) gives an introduction to the neutral atmosphere and the time varying effects on the thermospheric and exospheric density. These time varying effects include solar rotation, solar cycle, diurnal variations, magnetic storms and substorms, gravity waves, winds and tides, and long-term climate change. Vallado (2007) gives an introduction to the basic variations in density as well as the most commonly used density models in orbit determination. Sabol and Luu (2002) give a summary of the drivers of atmospheric density variations and discuss some of the difficulties connected with the temporal resolution of various proxies utilized by the empirical density models. Marcos et al. (2003) supply an overview of research addressing the inaccuracies in modeling satellite drag.

Two primary categories of research exist to address the problems of modeling atmospheric density for satellite drag. The first category is dynamic calibration of the atmosphere (DCA) and the second is using accelerometers onboard satellites to measure non-conservative accelerations, which includes drag. DCA utilizes the observed motions of a large number of satellites in order to estimate large-scale density corrections to an existing atmospheric density model (Bowman et al., 2007; Bowman, 2004; Cefola et al., 2003; Storz et al., 2005; Wilkins et al., 2007a, 2007b; Yurasov et al., 2004; Yurasov et al., 2008). Dynamic calibration of the atmosphere provides a significant improvement to empirical density models but with several disadvantages. First, a DCA approach is designed to run internal to a particular orbit determination scheme with the resulting atmospheric density corrections only applying to a specific time period. Therefore, those using a different orbit determination scheme must rely on that particular system for updates to atmospheric density corrections as well as requiring a complete archive of density corrections for a given problem. The second limitation of DCA approaches is the limited spatial and temporal resolution of the atmospheric density corrections. The corrections allow the baseline density model to characterize atmospheric density variations in terms of several hours to days but not in shorter time scales. A temporal limitation is introduced by the use of a daily solar flux and averaged 3-hour geomagnetic indices as input values into a DCA scheme. The use of this input data does not permit the baseline atmospheric density model to properly represent variations that occur within the averaging interval of these indices. Further difficulty arises in DCA approaches because of the predominate use of two-line element sets of a large number of low Earth orbit objects as observational inputs for a given DCA approach. Reliance on two-line elements results in reduced accuracy density corrections with restricted temporal resolution. The High Accuracy Satellite Drag Model (HASDM) (Storz et al., 2005) utilizes radar observations of low Earth orbit objects, but the accuracy of radar observations is still lower than those obtained by precision orbit ephemerides (POE) or satellite laser ranging (SLR). In addition, the radar observation data are not generally available.

The second category of research for improving atmospheric density knowledge is using accelerometers onboard satellites to measure non-conservative accelerations, which can be utilized to estimate density. The accelerometer data allows the separation of gravitational forces from non-conservative forces including Earth radiation pressure, solar radiation pressure, and drag. Use of accurate radiation pressure models permits the drag acceleration and resulting estimated density to be accurately calculated with precise temporal resolution. The accelerometer data are extremely precise but only available for a few satellites. This represents an extreme opposite in terms of accuracy and data availability compared with the use of two-line element sets. The availability of accelerometer measurements is currently limited to the Challenging Mini-Satellite Payload (CHAMP) and the two Gravity Recovery and Climate Experiment (GRACE) satellites. Other satellites with accelerometers have flown in the past. An example is given in

Rhoden et al. (2000), in which the accelerometer data from the Satellite Electrostatic Triaxial Accelerometer (SETA) experiment flown at an altitude of about 200 km was used to examine thermospheric density and confirmed that energy from magnetic storms deposited at high latitudes created a "density bulge" that propagated toward the equator and then toward the opposite poles.

Konig and Neumayer (2003) and Bruinsma and Biancale (2003a, 2003b) published some of the early results for estimating density using CHAMP accelerometer data with additional atmospheric density values derived using CHAMP accelerometer data by Bruinsma et al. (2004) and Nerem et al. (2003). Schlegel et al. (2005) examined polar region density structures by using CHAMP accelerometer data. Joint work between researchers at the University of Colorado and the Centre National d'Études Spatiales (CNES) utilized CHAMP and GRACE accelerometer data to examine density variations created during solar and geomagnetic events (Bruinsma et al., 2006; Bruinsma and Forbes, 2007; Forbes et al., 2005; Sutton et al., 2005; Sutton et al., 2006; Sutton et al., 2007). Tapley et al. (2007) describe a technique to estimate atmospheric density from the GRACE accelerometer data. The CHAMP and GRACE satellites have contributed vast amounts of information regarding the upper atmosphere and are capable of adding even more. Unfortunately, these three satellites only provide limited spatial coverage at any given time and only at low altitudes.

The research presented in this report is another step toward the goal of combining accurate data with good spatial coverage obtained from a large number of satellites. Many satellites currently possess Global Positioning System (GPS) receivers that when combined with precision orbit determination provide position accuracies of a few centimeters to within a few meters. This research estimates atmospheric density by using the precision orbit data of these satellites in a precision orbit determination scheme. CHAMP and GRACE POEs are used to estimate atmospheric density. Use of POE data results in increased accuracy from a smaller number of satellites as compared with two-line element sets. When compared with accelerometer data, POE data provide a larger number of available satellites with reduced accuracy. Several papers have examined the use of GPS receiver or SLR observations for estimating non-conservative accelerations. One such approach is given by Doornbos et al. (2005), where a type of differential correction was examined by using two-line element sets in a traditional DCA scheme along with a small number of satellites with precision orbit data. Another approach described as GPS accelerometry, utilizes GPS receiver data to estimate non-conservative forces as empirical accelerations (van den Ijssel et al., 2005; van den Ijssel and Visser, 2005, 2007). Through this method the in-track and cross-track accelerations derived from the CHAMP accelerometer may be reasonably determined with a temporal resolution of 20 minutes or greater. Montenbruck et al. (2005) utilized batch and Kalman filter estimation techniques in order to investigate the reconstruction of empirical accelerations of the GRACE-B satellite. Both the batch and Kalman techniques demonstrated similar overall variations in the empirical accelerations, but with a scale difference between the acceleration magnitudes obtained from the two methods. Willis et al. (2005) used Doppler Orbitography and Radiopositioning Integrated by Satellite (DORIS) and SLR data to examine density variations in the 800-900 km and 1300-1400 km ranges in the thermosphere during periods of enhanced geomagnetic activity. The study found significant errors in the atmospheric models, but these errors were greatly reduced with additional enhanced data processing. DORIS is yet another way of obtaining highly accurate satellite state vectors, and allows for formulation of corrections to atmospheric density models.

2.2 Methodology

The results presented in this paper were generated by processing the positions and velocities from the CHAMP and GRACE POE data as observations in an optimal orbit determination process in order to estimate density and ballistic coefficient. The POE data are available as rapid science orbits (RSO) and may be downloaded from the website http://isdc.gfz-potsdam.de. Konig et al. (2002, 2005, 2006) and

Michalek et al. (2003) discuss the processing and accuracy of the RSOs. The published accuracy of the RSOs compared to SLR data is 5-10 cm.
Atmospheric density is estimated as a correction to a baseline atmospheric density model as part of an orbit determination scheme using Orbit Determination Tool Kit (ODTK). The POE data are input as measurements into a sequential measurement processing and filtering scheme. A smoother is then applied to the filtered solution to account for all available solution data to increase the accuracy over the whole solution span. The filter and smoother combination estimates the time variable density and ballistic coefficient including realistic covariance matrices established by the physics associated with the problem. A 90x90 GRACE Gravity Model 2 (GGM02C) (Tapley et al., 2005), solar radiation pressure, Earth infrared and albedo radiation pressure, luni-solar point masses, general relativity, and solid Earth and ocean tides are force models in addition to drag included in the orbit determination process. SRP was modeled assuming CHAMP and GRACE were spheres with area of 6.5 m^2, which represents an averaged area. Earth infrared and albedo radiation pressure models assumed a constant area of 20 m^2, where the difference from the SRP area accounts for the larger area projected toward Earth for CHAMP and GRACE. Perfect absorption was assumed as a baseline for the radiation pressure modeling, but the coefficients are estimated. SRP is about two orders of magnitude lower than drag for the CHAMP altitude so these simplified models should introduce minimal error (Bruinsma et al., 2004). Process noise was only included for the gravity model. Since covariance information is not available for GGM02C, the process noise level was determined using Joint Gravity Model 2 (JGM2) (Nerem et al., 1994) error levels for low Earth orbit satellites. This is the default setting in ODTK. This is a conservative process noise level for the gravity model since the JGM2 errors are larger than the GGM02C errors. The POE observations were provided every 30 s and given a noise level of 10 cm.

Wright (2003) and Wright and Woodburn (2004) outline techniques for estimating density that are available in ODTK software package, which was used for this research. The technique permits the local atmospheric density to be estimated in real-time in conjunction with the orbit determination process and provides a significant improvement over the standard technique of estimating the ballistic coefficient (BC) or drag coefficient because BC estimates absorb the errors generated by the model for atmospheric density and BC. Additionally, BC estimates will often include geopotential model errors. Tanygin and Wright (2004) present the polynomial spline fit technique for geomagnetic indices utilized in the orbit determination scheme.

The estimated atmospheric density is obtained as a correction to an atmospheric model. The models available in ODTK are Jacchia 1971 (Jacchia, 1971), Jacchia-Roberts (Roberts, 1971), CIRA 1972 (COSPAR Working Group IV, 1972), MSISE-1990 (Hedin, 1991), and NRLMSISE-2000 (Picone et al., 2002). The Jacchia-Roberts and CIRA 1972 density models were derived from the Jacchia 1971 model so the results from these three models should be similar and these will be classified as the Jacchia models. Once a baseline atmospheric density model is selected, two different types of corrections are applied to the model as part of the orbit determination process. The first is a baseline correction derived from historical F10.7 and a_p measurements obtained over several solar cycles. The baseline density correction propagates from perigee height through the use of an exponential Gauss-Markov sequence. Error in the atmospheric density at perigee is related to the current point in the orbit through a transformation internal to ODTK.

The second type of atmospheric density correction utilizes the observations and current conditions to yield a dynamic correction. The use of a sequential process allows a correction to be estimated at each time step in the filter as opposed to a single correction applied to the complete time span of data or many corrections increasing the size of the state for a batch least squares process.

Exponentially correlated Gauss-Markov processes describing the modeling errors also exist for dynamic corrections as observed for the baseline corrections. The user of the optimal orbit determination process

may specify the values of the density and ballistic coefficient exponential Gauss-Markov process half-lives, which determines the effect of past data on the individual density correction at each time step. While the ballistic coefficient is estimated as part of the filter/smoother process, the ballistic coefficient was initialized using yearly averages of 0.00444 m^2/kg for 2002-2003 and 0.00436 m^2/kg for 2004-2005 (Bowman et al., 2008). Values for the CHAMP satellite's nominal ballistic coefficient that were not included in these years were estimated for years both preceding and following these ranges by taking into account the changing mass of the satellite (Hiatt, 2009). The nominal ballistic coefficient for GRACE is defined as 0.00687 m2/kg in the ODTK orbit determination scheme (Bowman et al., 2008).

The derived densities obtained from the POE data are compared against those derived from the CHAMP accelerometer as calculated by Sean Bruinsma of CNES. Bruinsma's density values are averaged to 10-second intervals. POE derived density solutions were developed for multiple time periods with varying levels of solar and geomagnetic activity. The authors have used geomagnetic and solar activity bins defined based on Picone et al. (2002) to establish low solar activity as defined by $F10.7 < 75$, moderate solar activity for $75 \leq F10.7 < 150$, elevated solar activity for $150 \leq F10.7 < 190$, and high solar activity by $F10.7 \geq 190$. Additionally, quiet geomagnetic periods are defined for $A_p \leq 10$, moderate geomagnetic activity for $10 < A_p < 50$, and active geomagnetic periods by $A_p \geq 50$. These definitions are applied to separate the POE derived density solutions into the appropriate categories. This cataloging of solutions facilitates the analysis of the POE derived density solutions as a function of solar and geomagnetic activity.

2.3 Initial CHAMP Results and Calibration

McLaughlin and Bieber (2007) presented the initial results of estimating density using CHAMP POE. The paper found densities estimated using different baseline density models and densities estimated in overlap regions to be consistent within 10 percent. McLaughlin et al. (2008a) made the first comparisons of CHAMP POE derived atmospheric densities to those derived from the accelerometer data and found errors bounded within about 10 percent for days with moderate solar and geomagnetic activity. Follow-on work focused on calibrating the POE derived densities using the accelerometer derived densities. McLaughlin et al. (2008b, 2011b), Hiatt et al. (2009), and Hiatt (2009) presented initial calibration results for CHAMP and showed that density and ballistic coefficient half-lives of 1800 and 180,000 minutes did not perform well in estimating density. Therefore, further work focused on half-lives of 1.8, 18, or 180 minutes. These works also showed that POE derived corrections to Jacchia based density models matched the accelerometer derived densities better than POE derived corrections to MSIS based density models did. Lechtenberg (2010) included a more comprehensive examination of CHAMP POE derived densities and examined days from 2001 to 2007 picked so that the distribution of solar and geomagnetic activity level bins matched those over all days from the launch of CHAMP through 2007 and so that days from different times in the year were adequately represented. The results of this study are summarized in Table 1 including the best density half-life, ballistic coefficient half-life, and baseline density model combination. The best combination was determined based on both cross correlation and RMS. The different Jacchia based density models had nearly identical results, especially for cross correlation.

These results show the very high correlation between CHAMP POE and accelerometer derived densities and relatively low RMS differences. The consistently best combination included a ballistic coefficient half-life of 1.8 minutes and a CIRA 1972 baseline density model. In addition, 180 minutes was usually the best half-life for density. The differences between density found with 18 and 180 minute half-lives for density was usually negligibly different.

Table 1: Best Combinations for CHAMP POE-Derived Density Correlation and RMS with Accelerometer-Derived Density.

Bin	Density Half-Life (min)	BC Half-Life (min)	Atmospheric Model	Cross Correlation	RMS (10^{-12} kg/m^3)
Overall	180	1.8	CIRA 1972	0.910	0.570
Quiet Geomagnetic	180	1.8	CIRA 1972	0.955	0.348
Moderate Geomagnetic	180	1.8	CIRA 1972	0.919	0.464
Active Geomagnetic	18	1.8	CIRA 1972	0.856	0.960
Low Solar	180	1.8	CIRA 1972	0.931	0.296
Moderate Solar	180	1.8	CIRA 1972	0.893	0.559
Elevated Solar	18	1.8	CIRA 1972	0.947	0.581
Active Solar	180	1.8	CIRA 1972	0.906	0.759

2.4 CHAMP and GRACE Calibration

Fattig et al. (2010), Fattig (2011), and McLaughlin et al. (2013) presented the first extensive calibration that examined the same days for CHAMP and GRACE to see if the best parameters were consistent between CHAMP and GRACE. These studies included days from the launch of GRACE in 2004 through 2009. No elevated or high solar activity days occurred during this time period. Table 2 shows a summary of the results for CHAMP and Table 3 shows a summary of the GRACE results.

Tables 2 and 3 show that the results are fairly consistent between the CHAMP and GRACE orbits and across solar and geomagnetic activity levels. Again the overall best combination was with corrections to a Jacchia-based model. Ballistic coefficient half-life was best at 1.8 minutes and the density half-life was best at 18 or 180 minutes with the difference between the densities estimated with the two density half-lives being small.

Table 2: Best Combinations for CHAMP POE-Derived Density Correlation and RMS with Accelerometer-Derived Density.

Bin	Density Half-Life (min)	BC Half-Life (min)	Atmospheric Model	Cross Correlation	RMS (10^{-12} kg/m^3)
Overall	18	1.8	CIRA 1972	0.883	0.623
Quiet Geomagnetic	180	1.8	CIRA 1972	0.936	0.272
Moderate Geomagnetic	180	1.8	CIRA 1972	0.945	0.418
Active Geomagnetic	18	1.8	CIRA 1972	0.818	0.961
Low Solar	180	1.8	CIRA 1972	0.928	0.264
Moderate Solar	18	1.8	CIRA 1972	0.868	0.761

Table 3: Best Combinations for GRACE POE-Derived Density Correlation and RMS with Accelerometer-Derived Density.

Bin	Density Half-Life (min)	BC Half-Life (min)	Atmospheric Model	Cross Correlation	RMS (10^{-12} kg/m^3)
Overall	180	1.8	Jacchia-Roberts	0.849	0.123
Quiet Geomagnetic	180	1.8	Jacchia 1971	0.802	0.037
Moderate Geomagnetic	180	1.8	Jacchia-Roberts	0.912	0.076
Active Geomagnetic	180	1.8	Jacchia-Roberts	0.845	0.207
Low Solar	180	1.8	Jacchia 1971	0.766	0.030
Moderate Solar	180	1.8	Jacchia-Roberts	0.883	0.160

McLaughlin et al. (2009) and Mehta and McLaughlin (2011) examined the simultaneous ballistic coefficient and density estimation. The estimated density magnitude is sensitive to the nominal ballistic coefficient selected so a bias in nominal ballistic coefficient does lead to a bias in the estimated density. Therefore, ballistic coefficient and density are not completely separable without a good knowledge of what the average ballistic coefficient should be. The estimated ballistic coefficients show a 3-5% percent variation in magnitude with a cycle of roughly twice per orbit. For CHAMP, the correlation between the density error, defined as the difference between accelerometer and POE derived densities, and the ballistic coefficient was around -0.3 for ballistic coefficient half-life of 1.8 min and density half-life of 18 min and near zero if density half-life was increased to 180 min. For GRACE the correlation for the density half-life of 180 min was 0.1 with other results about the same as for CHAMP. If ballistic coefficient error was being absorbed by the density estimation, one would expect a high negative correlation between these two quantities. However, some ballistic coefficient error is almost certainly being absorbed in the density estimates, but the effects on the density estimation are small based on comparisons with the accelerometer. These papers also examined the effects of fixing ballistic coefficient at the nominal value and showed that the difference in density is small between estimating and not estimating the ballistic coefficient.

Based on the density and ballistic coefficient studies, nominal settings were used for further analysis. The nominal settings were CIRA 1972 as the baseline density model, ballistic coefficient half-life of 1.8 minutes, and density half-life of 180 minutes. An additional benefit of 180 minute half-life compared to the 18 minute half-life is that it provides an additional order of magnitude difference between the ballistic coefficient and density half-lives. Large separation between density and ballistic coefficient half-lives was a condition for the two factors to be simultaneously observable (Wright, 2003; Wright and Woodburn, 2004).

2.5 Continuous Density Data Sets and Accuracy Comparisons

Mysore Krishna and McLaughlin (2011) and Mysore Krishna (2012) presented the technique used to combine 14 hour density solutions into a continuous density data set over the life of CHAMP and from launch through 2011 for GRACE. The data are available as one week data sets to keep the individual file sizes manageable. The method used to merge the data is the linear weighted blending technique (Kim, 2008; Kim et al., 2008; Kim et al., 2009). The technique applies weights to overlapping areas of the fourteen day density solution based on how far the point is from the end or beginning of the overlapping solution. The 14 hour solutions have two hour overlaps so at the beginning of the two hour overlap the combined density will match the density of the earlier of the two fourteen hour solutions; at the midpoint of the overlap region the combined density will be a straight average of the two densities; and at the end of the overlap region the combined density will match the density of the latter of the two fourteen hour solutions. The primary value of this technique is to provide a smooth solution, but it also gives more weight to points farthest from the endpoint of a given solution. This is valuable since for an orbit solution one would typically expect the points at the end a given solution to be of lower accuracy than points closer to the middle. Effectively, this technique uses information from the other overlapping solution to provide more information about what is happening in the overlap regions.

Cross correlation and RMS of the HASDM, POE derived, NRLMSISE-00, and Jacchia 71 densities with accelerometer derived densities were calculated and compared for both CHAMP and GRACE. Table 4 contains the cross correlation coefficients of the POE derived density, HASDM densities, and of the Jacchia 71 model compared to accelerometer derived density for the various levels of solar and geomagnetic activity as well as for the entire mission life. The RMS comparisons are contained in Table 5. The tables show the POE derived density matches the accelerometer density significantly better than Jacchia 71 and NRLMSISE-00 both overall and for every level of solar and geomagnetic activity. The POE derived density is also moderately better than the HASDM density for all conditions. CHAMP is

included as a satellite in the HASDM solutions so the HASDM densities for CHAMP are likely better than for a satellite not included in the HASDM solutions.

Table 4: Cross correlation coefficients for POE derived density, HASDM, NRLMSISE-00, and Jacchia 71 with accelerometer derived density along the CHAMP orbit.

Bin	Cross Correlation			
	POE derived density	HASDM	NRLMSISE-00	Jacchia-71
Overall	0.934	0.924	0.888	0.886
Low Solar	0.926	0.910	0.880	0.884
Moderate Solar	0.935	0.925	0.881	0.884
Elevated Solar	0.938	0.936	0.907	0.895
High Solar	0.948	0.942	0.903	0.895
Quiet Geomagnetic	0.935	0.923	0.891	0.896
Moderate Geomagnetic	0.932	0.924	0.885	0.874
Active Geomagnetic	0.950	0.941	0.871	0.831

Table 5: RMS for POE derived density, HASDM, NRLMSISE-00, and Jacchia 71 with accelerometer derived density along the CHAMP orbit.

Bin	Root Mean Square (10^{-12} kg/m^3)			
	POE derived density	HASDM	NRLMSISE-00	Jacchia-71
Overall	0.383	0.400	0.701	0.836
Low Solar	0.322	0.346	0.849	0.925
Moderate Solar	0.354	0.372	0.643	0.663
Elevated Solar	0.526	0.531	0.719	1.027
High Solar	0.573	0.576	0.783	1.434
Quiet Geomagnetic	0.346	0.361	0.745	0.759
Moderate Geomagnetic	0.423	0.441	0.658	0.895
Active Geomagnetic	0.925	0.986	0.551	3.231

Table 6 shows the cross correlation and Table 7 shows the RMS results for GRACE. No elevated or high solar activity days or active geomagnetic weeks occurred during the available GRACE POE data (starting in 2004). The trends are very similar to those observed in the CHAMP data. Once again the POE derived density is clearly superior to the Jacchia 71 and NRLMSISE-00 models and slightly better than HASDM in matching the accelerometer derived density. These results show the promise of POE derived density from many satellites to improve the overall knowledge of density in the thermosphere.

Table 6: Cross correlation coefficients for POE derived density, HASDM, NRLMSISE-00, and Jacchia 71 with accelerometer derived density along the GRACE orbit.

Bin	Cross Correlation			
	POE derived density	HASDM	NRLMSISE-00	Jacchia-71
Overall	0.885	0.873	0.844	0.839
Low Solar	0.855	0.840	0.822	0.816
Moderate Solar	0.912	0.902	0.863	0.859
Quiet Geomagnetic	0.883	0.869	0.852	0.840
Moderate Geomagnetic	0.891	0.881	0.827	0.836

Table 7: RMS for POE derived density, HASDM, NRLMSISE-00, and Jacchia 71 with accelerometer derived density along the GRACE orbit.

Bin	Root Mean Square (10^{-12} kg/m^3)			
	POE derived density	HASDM	NRLMSISE-00	Jacchia-71
For all Bins	0.044	0.047	0.089	0.111
Low Solar	0.031	0.031	0.079	0.100
Moderate Solar	0.056	0.060	0.098	0.122
Quiet Geomagnetic	0.036	0.038	0.080	0.096
Moderate Geomagnetic	0.063	0.068	0.109	0.147

Figure 1 shows the cross correlation of CHAMP POE derived and HASDM densities with accelerometer derived densities and the angle between the CHAMP orbit plane and the Sun vector, β, from 2001 to 2008. Figure 2 shows the same for GRACE. Both figures show a periodic variation in correlation for both POE and HASDM densities where the lower correlation occurs where β is near zero. This occurs when the orbit plane is near the terminator. The reason for the lower correlation is that the normal daylight/darkness variation that dominates the signal is much lower in amplitude when the orbit plane is near the terminator. When this happens the high frequency density variations that are only observed by the accelerometer are of the same order as the daylight/darkness variations, which brings the correlations down. This is discussed more fully in McLaughlin et al. (2011a).

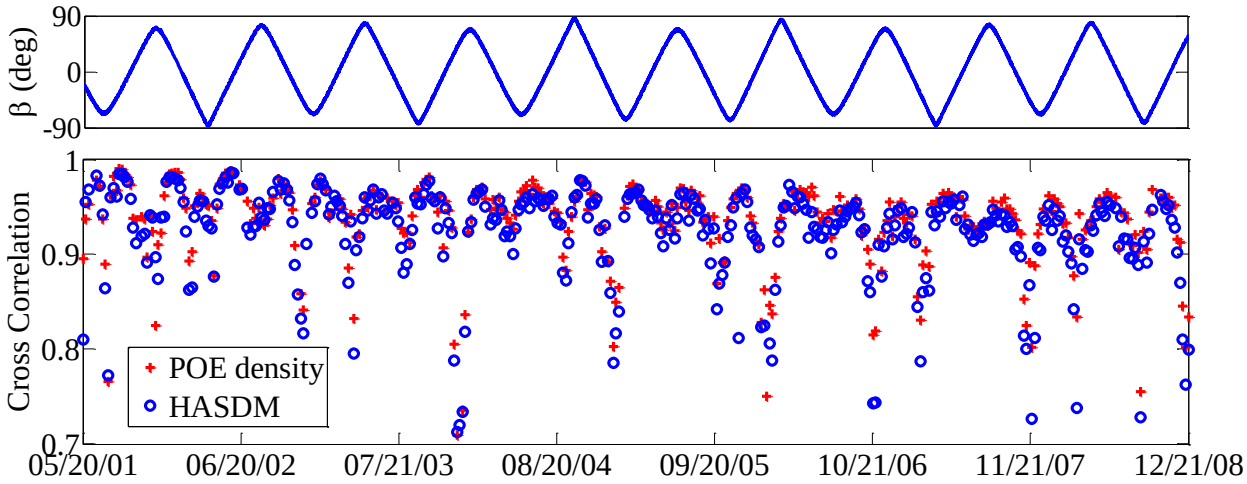

Figure 1: Beta angle and weekly cross correlation between POE and HASDM densities with accelerometer densities for CHAMP.

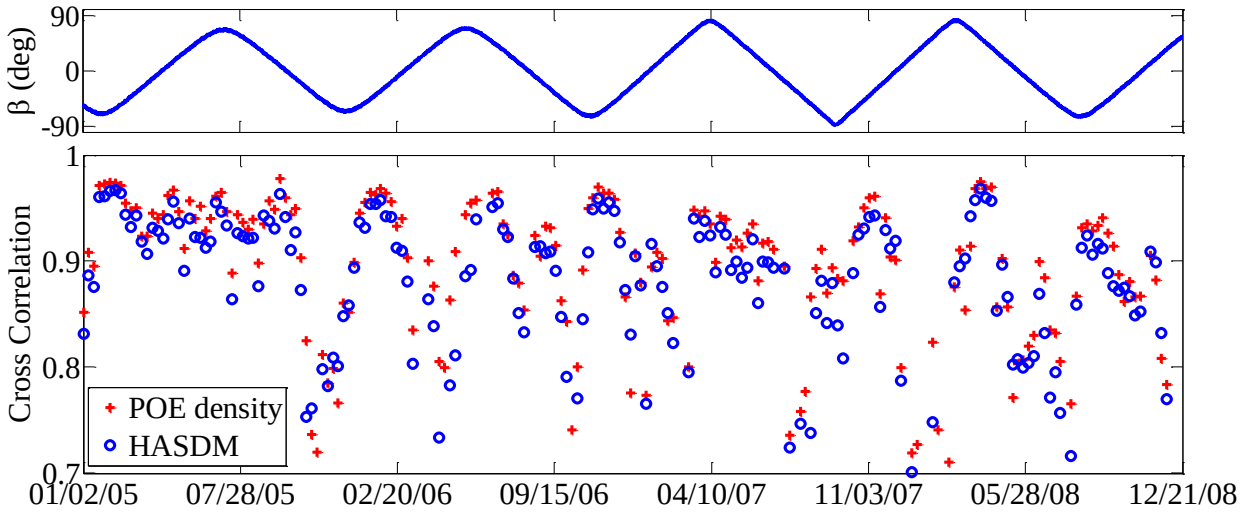

Figure 2: Beta angle and weekly cross correlation between POE and HASDM densities with accelerometer densities for GRACE.

2.6 Comparison of Density Estimation from Multiple Satellites

Interesting times to compare the density found from the CHAMP and GRACE satellites are when the satellites' orbits are nearly coplanar. One such time occurred during April of 2005. Of particular interest is when GRACE is flying nearly directly above CHAMP because the density differences can be attributed solely to altitude. For the April 2005 coplanar period this condition was met for a few hours about every two days including on April 3 and April 5. Solar activity was at moderate levels on both days. Geomagnetic activity was low on April 3 and right on the moderate/active border on April 5. However, a geomagnetic storm occurred on late April 4, extending into early April 5 where a_p peaked at 132 early on April 5. This geomagnetic activity is apparent in the data for April 5. The analysis used CIRA 1972 as the baseline density model, BC half-life of 1.8 min, and density half-life of 180 min for both CHAMP and GRACE POE densities.

Figure 3 shows the densities for CHAMP and GRACE-A for April 3, 2005 found from the accelerometer, from HASDM, from Jacchia 1971, from precision orbit ephemerides (POE), and from NRLMSISE-00. Because of the higher altitude, GRACE densities are an order of magnitude lower than the CHAMP densities, but the overall structure is similar between the satellites for each individual data set. Interesting features observable in the accelerometer data are nocturnal peaks in density that occur for both satellites between the major diurnal peaks that occur during the sunlit portion of the orbit. These nocturnal features are not observable in most of the other data sources except for some very slight humps or elevated density troughs during the times of the nocturnal peaks. However, NRLMSISE-00 does model these peaks, but for GRACE often has a secondary peak that does not appear in the accelerometer data. The nocturnal peaks occur over the equator and correspond to the Midnight Density Maximum (MDM) discussed in Arduini et al. and Akmaev et al. Both the POE and HASDM densities match the accelerometer very well for the CHAMP satellite, but the Jacchia 1971 and NRLMSISE-00 models tend to overestimate peak density. For GRACE all other data sources overestimate the sunlit peaks seen in the accelerometer data.

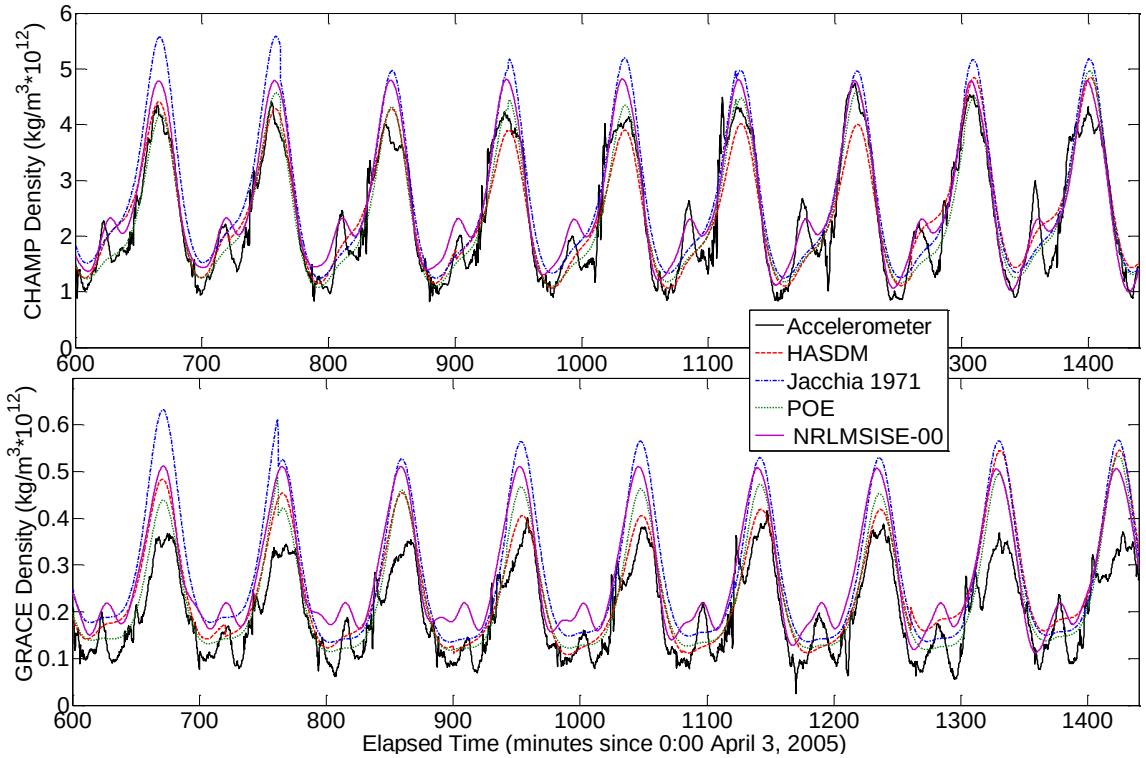

Figure 3. Densities Measured and Estimated for the CHAMP and GRACE-A Satellites on April 3, 2005.

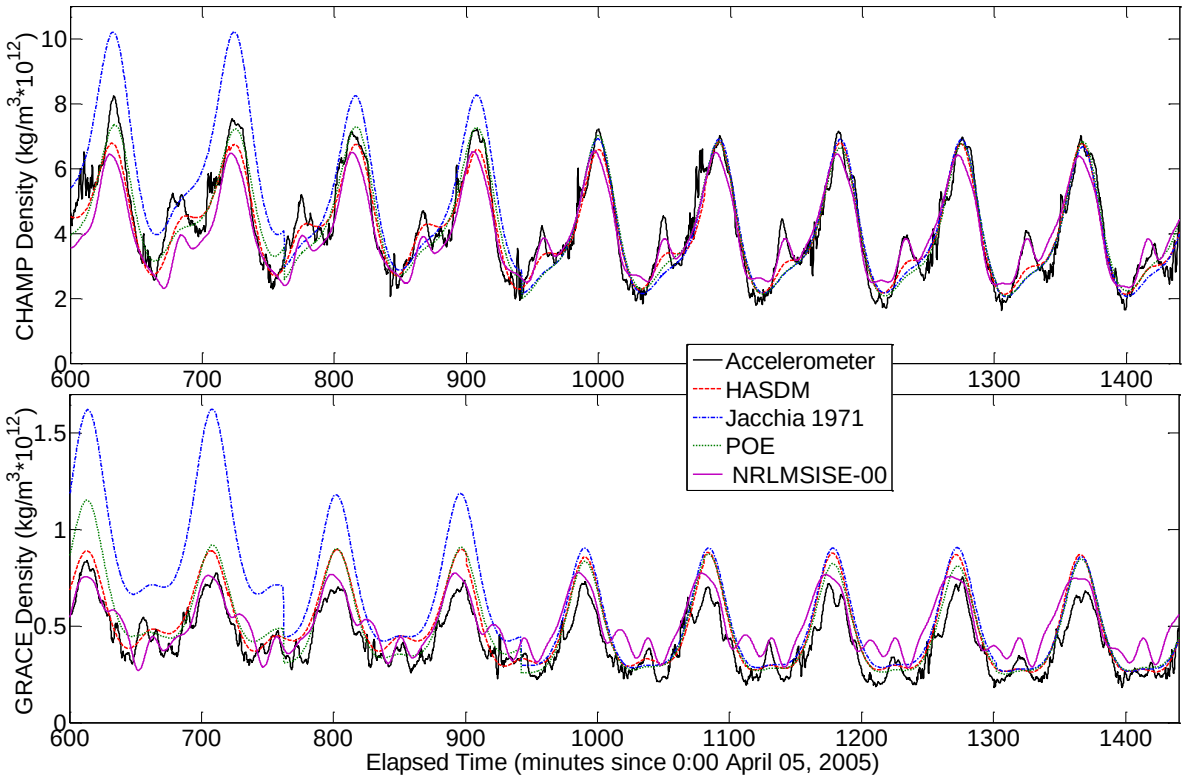

Figure 4. Densities Measured and Estimated for the CHAMP and GRACE-A Satellites on April 5, 2005.

Figure 4 shows data similar to Figure 3 for the next time period when GRACE is nearly directly above CHAMP on April 5, 2005. The density magnitudes are approximately double what they were on April 3. This increase is caused by the geomagnetic storm that began on late April 4 as discussed earlier. The early part of this time period shows an overestimation of atmospheric density by Jacchia 1971 caused by the elevated geomagnetic indices earlier in the day. The densities for both CHAMP and GRACE gradually decline to lower values over the course of this time period. Again, both CHAMP and GRACE accelerometer densities observe MDM not well observed in the other data sources except NRLMSISE-00. HASDM and the POE densities both match the accelerometer densities very well for CHAMP, but not as well for GRACE. NRLMSISE-00 does quite well for this time period except for the extra peaks appearing for GRACE.

This subsection also examines densities estimated from CHAMP, GRACE, and TerraSAR-X for the period of September 21-30, 2007. During this period, CHAMP had an altitude of about 360 km, GRACE had an altitude of about 473 km, and TerraSAR-X had an altitude of about 528 km. Simultaneous density estimation for the three satellites shows atmospheric activity at multiple altitudes in the atmosphere. CIRA 1972 was used as the baseline density model with 180 min for the density half-life and 1.8 min for the ballistic coefficient half-life for all satellites.

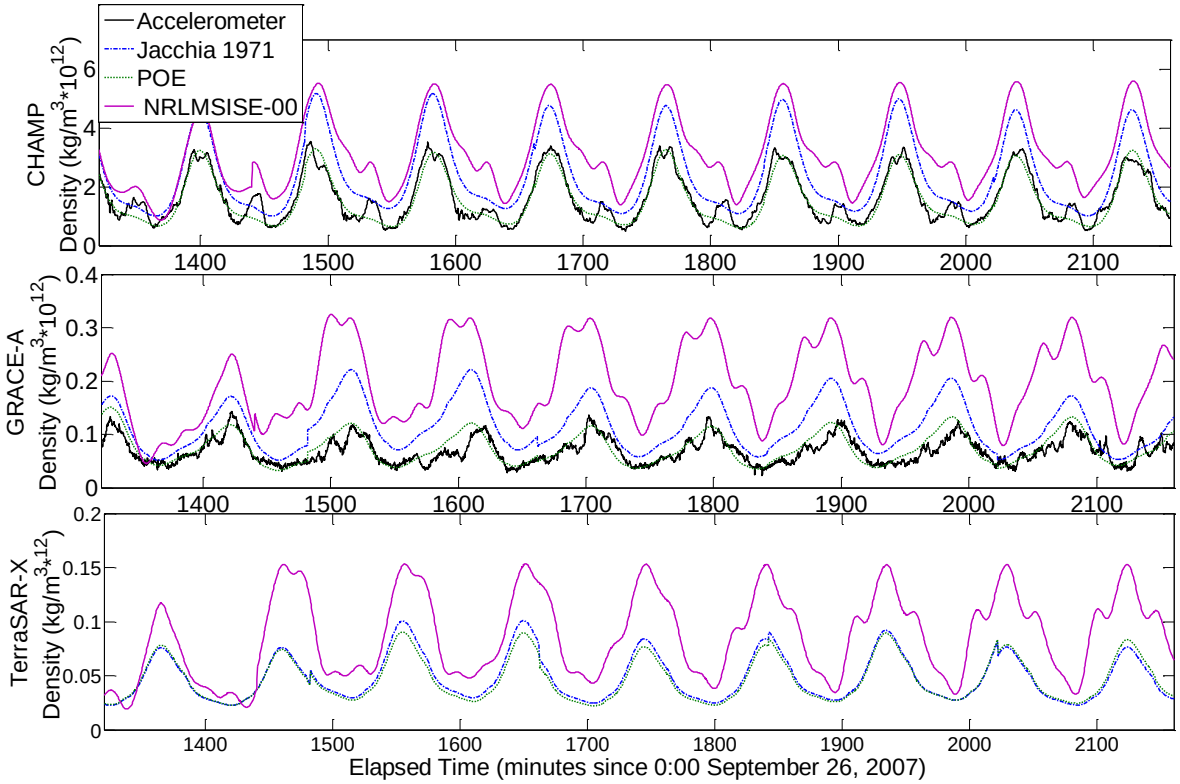

Figure 5. Estimated and Measured Densities for CHAMP, GRACE, and TerraSAR-X, September 26-27, 2007.

Figure 5 shows the POE, Jacchia 1971, and NRLMSISE-00 densities for CHAMP, GRACE, and TerraSAR-X; and the accelerometer densities for CHAMP and GRACE for a 14 hour solution from September 26 to September 27, 2007. Solar activity level was low on both days and geomagnetic activity was low on the 26th and moderate on the 27th. CHAMP densities are more than an order of magnitude greater than GRACE densities and TerraSAR-X densities are about half of GRACE densities. The MDM seen in the previous section are apparent in the CHAMP accelerometer data, but do not appear in the POE density. These peaks are also no longer readily observable in the GRACE accelerometer derived densities. However, GRACE is not flying nearly directly above CHAMP as in the previous section.

Aside from these peaks and some other short period variations, the POE density matches the accelerometer density very well. NRLMSISE-00 and Jacchia 1971 significantly overestimated the density for both CHAMP and GRACE compared to the accelerometer and POE density. For TerraSAR-X the POE density is very near Jacchia 1971. This could be caused by either Jacchia 1971 better modeling the density at this higher altitude or the POE technique having increased difficulty observing density variations at higher satellite altitudes and lower density magnitudes. Although not shown in the figure, the POE density derived as corrections to NRLMSISE-00 for TerraSAR-X was close to the POE density derived from CIRA 1972 that is shown in the figure.

Figure 6 shows data similar to Figure 5 for 14 hours from September 29 to 30, 2007. Solar activity level was low on both days and geomagnetic activity was moderate on the 29th and 30th. The trends are similar, but the density magnitudes for all satellites are approximately double the values on September 26 and 27. The MDM are again seen in the CHAMP accelerometer densities, but are not well defined in GRACE. Jacchia 1971 again overestimates density for CHAMP and GRACE, but POE derived densities match the accelerometer very well. NRLMSISE-00 does very well for CHAMP, but overestimates the densities for GRACE. For TerraSAR-X the difference between POE and Jacchia 1971 densities is again much less distinct than for CHAMP and GRACE, but the values have greater separation than on September 26 and 27. This difference could be caused by higher overall density on the later days. NRLMSISE-00 and the POE densities match well for TerraSAR-X for the last half of this time span.

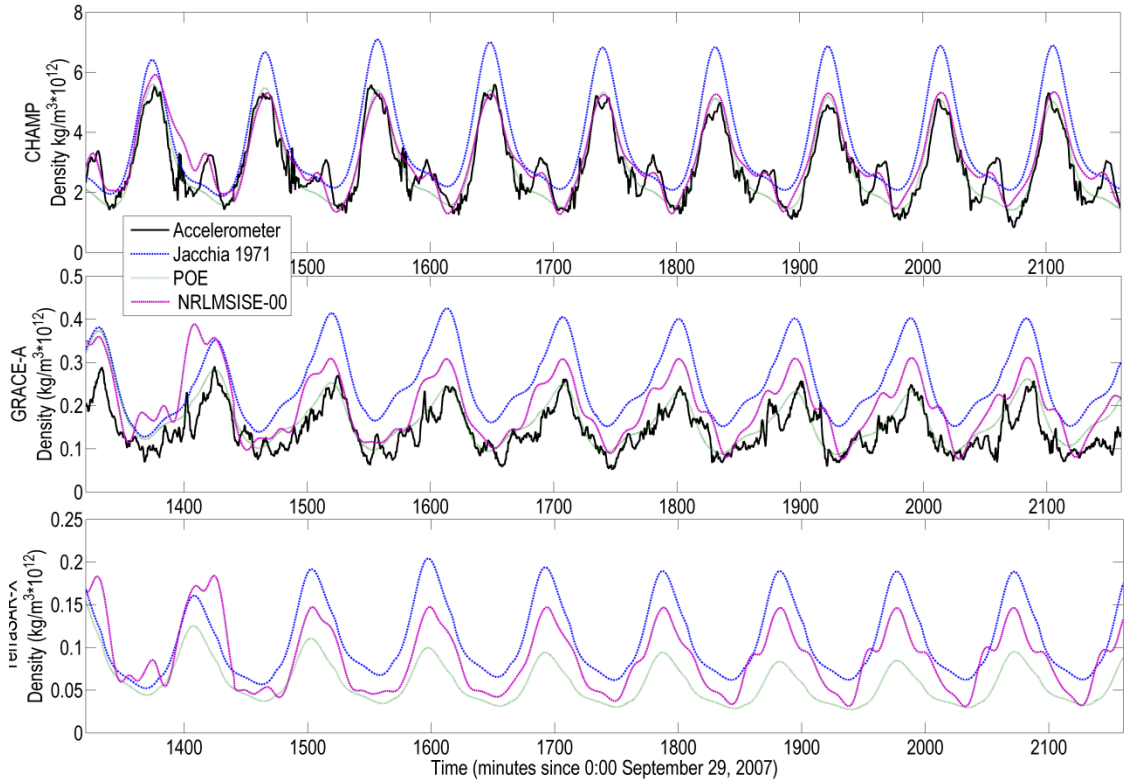

Figure 6. Estimated and Measured Densities for CHAMP, GRACE, and TerraSAR-X, September 29-30, 2007.

2.7 Effects of Orbit Ephemeris Error and Limited Data on Density Estimation

The previous work has focused on satellites with continuous data of high accuracy, which is only available from a limited number of satellites with high quality GPS receivers. The effects of limited data and lower quality data on density estimation are examined to see the suitability of using a larger set of

satellites to estimate density. Discontinuous data sets are created by decimating the original POE data for CHAMP and GRACE. This file is then used as an input in ODTK to obtain the POE derived density estimates.

The next step is to introduce different levels of ephemeris noise to the POE data and estimate density using the lower accuracy data. The effects reduced accuracy ephemeris data and its effect on density estimation was initially examined by Locke (2012). Noise levels of 0.1, 0.5, 1, 10, and 100 m were added to the data and data was decimated so that data existed for 15 and 8 minutes per orbit.

Tables 8 and 9 show the cross correlation results with 15 minutes of data per orbit for CHAMP and GRACE, respectively. As expected, the cross correlation goes down as the noise level is increased. However, the overall accuracy remains reasonably high even up to 100 m noise levels. The results for RMS and for 8 minutes per orbit show similar decreases in accuracy/precision and even with only eight minutes of data per orbit the density estimates remain usable for even relatively high noise levels.

Table 8. Cross correlation between POE derived density estimates and Bruinsma's accelerometer derived densities for the CHAMP orbit using various noise level data available 15 minutes per orbit

Bin	**Cross Correlation for various noise levels (m)**						
	Full Data	**0**	**0.1**	**0.5**	**1.0**	**10.0**	**100.0**
Overall	0.917	0.913	0.906	0.901	0.899	0.893	0.869
Low Solar	0.900	0.888	0.877	0.852	0.846	0.847	0.820
Moderate Solar	0.922	0.920	0.914	0.914	0.914	0.907	0.887
Elevated Solar	0.948	0.946	0.942	0.945	0.944	0.938	0.919
High Solar	0.890	0.880	0.877	0.876	0.876	0.857	0.811
Quiet Geomagnetic	0.937	0.934	0.927	0.921	0.920	0.916	0.900
Moderate Geomagnetic	0.892	0.888	0.881	0.877	0.875	0.867	0.829
Active Geomagnetic	0.855	0.841	0.838	0.838	0.838	0.821	0.784

Table 9. Cross correlation between POE derived density estimates and Bruinsma's accelerometer derived densities for the GRACE orbit using various noise level data available 15 minutes per orbit

Bin	Cross Correlation for various noise levels (m)						
	Full Data	**0**	**0.1**	**0.5**	**1.0**	**10.0**	**100.0**
Overall	0.862	0.825	0.820	0.813	0.813	0.815	0.813
Low Solar	0.708	0.598	0.601	0.587	0.588	0.603	0.620
Moderate Solar	0.901	0.886	0.874	0.875	0.875	0.871	0.854
Quiet Geomagnetic	0.850	0.808	0.807	0.794	0.797	0.795	0.802
Moderate Geomagnetic	0.861	0.827	0.817	0.823	0.818	0.826	0.837
Active Geomagnetic	0.831	0.813	0.808	0.787	0.784	0.776	0.689

3 Effects on Orbit Propagation

3.1 Background and Methodology

Some previous work has examined the effects of different frequency signals on orbit propagation. Anderson et al. (2009) studied the effects of different wavelength density perturbations and temporal resolution on orbit propagation. Schaeperkoetter and McLaughlin (2010) compared orbit propagations along the CHAMP orbit using accelerometer derived density to those using POE derived density and HASDM density for several generic time periods. However, neither of these works directly examines how specific types of high frequency signals seen in accelerometer derived densities affect orbit propagation. The effects have clear implications for the need to model these variations in future density models used in orbit analysis.

McLaughlin, Locke, and Mysore Krishna (2012) use a precision orbit initial vector and propagate the orbit using central body and J2 gravitation with drag using density from accelerometer, POE, HASDM, or Jacchia 71. The orbits using the different densities are compared for 24 hour propagation using both root mean square and maximum difference. This method does not account for how the difference in propagated position would give different model results. This is justified by assuming the density difference would be small.

A position and velocity vector is taken from the POE solutions to initialize the integration. The force models include Earth central body and oblateness (J2) geopotential, and drag. Orbits are propagated with density from the accelerometer, POE, HASDM, or Jacchia 71 and the resulting orbits are compared assuming the accelerometer derived density gives the truth orbit. Earth constants are from the WGS-84 model. The inverse ballistic coefficients are defined to be 0.00436 m2/kg for CHAMP and 0.00687 m2/kg for GRACE.

The POE, HASDM, and Jacchia 71 densities are normalized to the same mean as the accelerometer densities because the primary concern in this research is the effect of temporal variations on the orbit propagation and not on the bias between the density data sets or models. The normalization is performed

by dividing the POE derived, HASDM, or Jacchia 71 densities by their mean and multiplying by the mean of the accelerometer derived densities. The means used are those for each particular 24 hour period of propagation. This method of normalization was used assuming the bias between the data sets is caused by errors in the inverse ballistic coefficients used in solving for densities.

Accelerometer derived densities are given in ten second increments. The integrator step size was also ten seconds to ensure that the integration included all variations in density observed by the accelerometer.

3.2 CHAMP Orbit Propagations

Normal Day. Figure 7 shows the densities and orbit propagation results for a normal day for CHAMP. The densities in the figure are the actual model or derived densities that have not been normalized. The reason for plotting the densities before normalization is so the different density sources can be more easily observed in the figure. The POE derived densities clearly provide better orbit propagation accuracy than HASDM or Jacchia 71. The worst case error for the propagation with POE derived densities is only 13 m, which would not be significant for most applications.

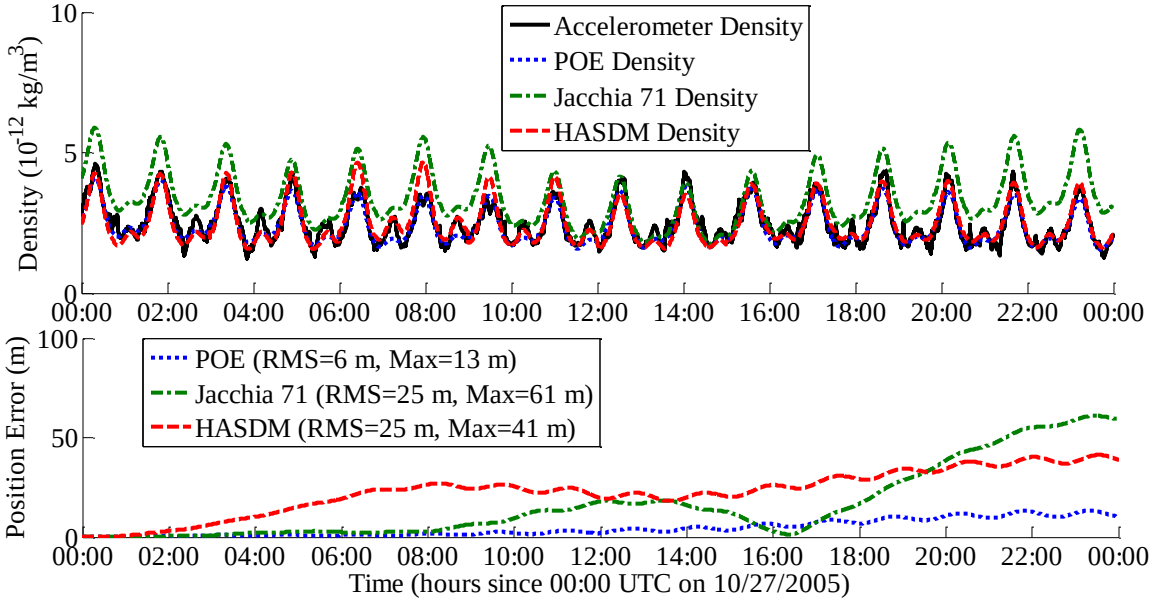

Figure 7. Density and orbit propagation errors along the CHAMP orbit on a normal day (October 27, 2005).

Traveling Atmospheric Disturbance. Figure 8 includes densities and orbit propagation errors for a day that includes a TAD, which is an increase in density caused by geomagnetic activity that begins at high latitudes and propagates toward the equator resulting in constructive interference between the waves near the equator. The TAD on April 19, 2002 occurs between 1100 and 1500 UTC and the resulting density enhancements can be observed in the figure. In addition, in the orbit propagation plot the direction of the drift caused by errors in the Jacchia 71 model changes at about this time. However, the errors in orbit propagation using the POE derived densities remain quite small. Clearly, the high frequency signals observed by the accelerometer, but not in the POE derived densities do not have a major effect on orbit propagation.

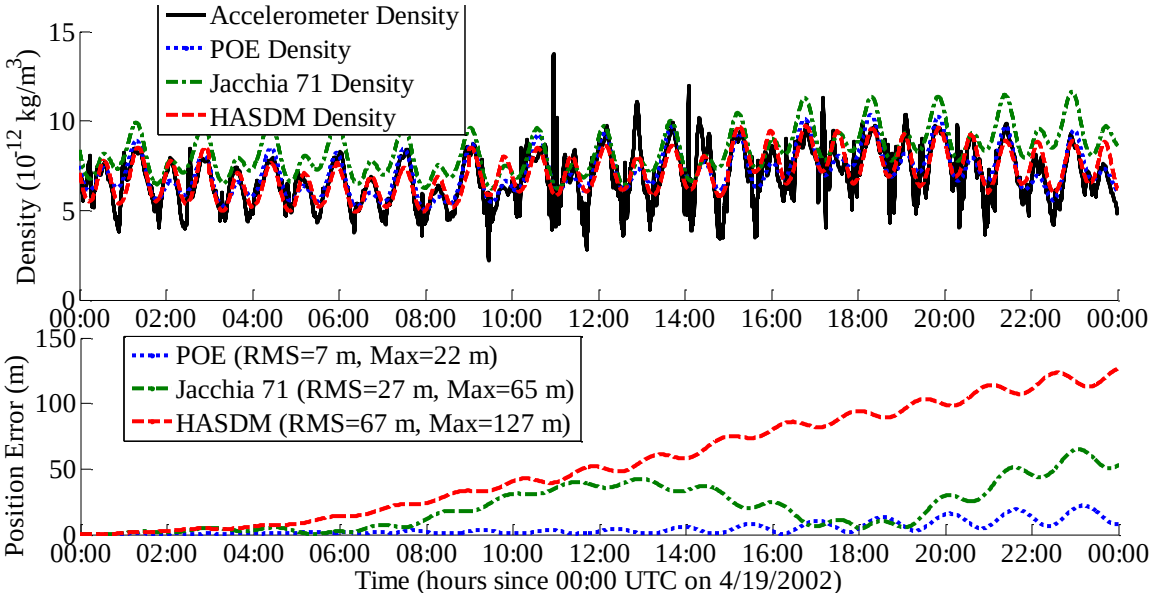

Figure 8. Density and orbit propagation errors along the CHAMP orbit on a day with a traveling atmospheric disturbance (TAD) (April 19, 2002).

Polar Cusp Density Enhancements. The accelerometer on CHAMP observed density enhancements that occurred around the polar cusp. The causes of these increases in density have been an active area of investigation. These are seen as spikes in density that occur on both sides of the magnetic pole, but are not always observable and not necessarily tied to increased geomagnetic activity. Figure 9 shows densities and orbit errors for March 21, 2002, which was a day on which polar cusp enhancements were observed. A small spike in the accelerometer density can be seen at this time, but no discernible effects are observed on any of the orbit propagations. The maximum error for the orbit propagation with the POE derived densities only reaches 8 m.

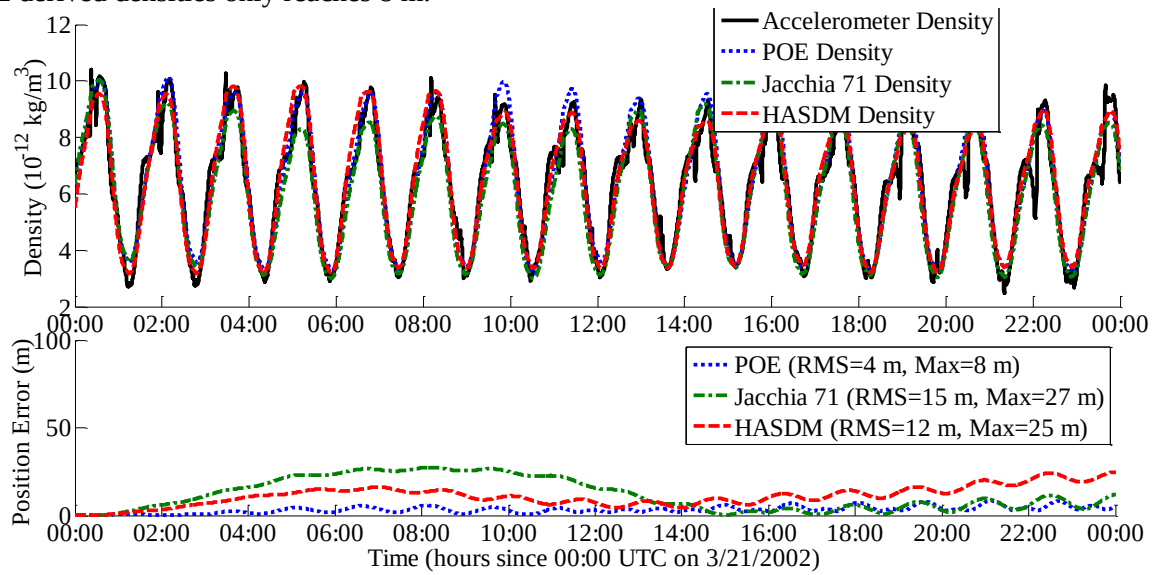

Figure 9. Density and orbit propagation errors along the CHAMP orbit on a day with a polar cusp density enhancement (March 21, 2002).

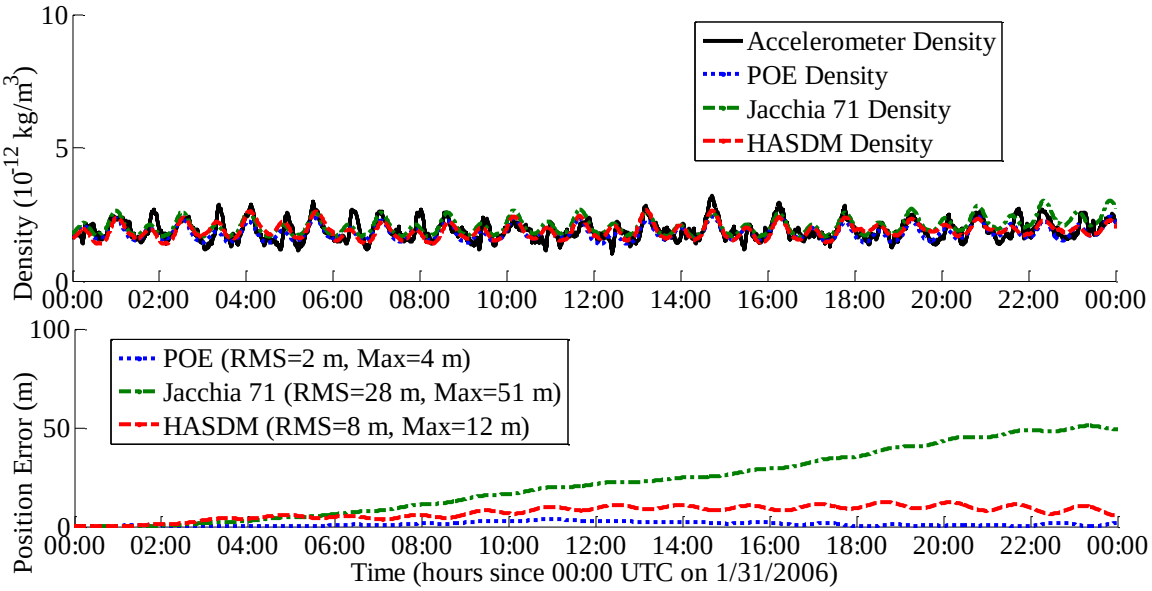

Figure 10. Density and orbit propagation errors along the CHAMP orbit on a day when the CHAMP orbit plane is near terminator (January 31, 2002).

Orbit Plane near the Terminator. When the orbit plane is near the terminator, the high frequency variations seen in the accelerometer derived densities can be of the same magnitude as the variations from the satellite traveling from daylight into darkness and back. This is because the normal variations are of much lower magnitude when the satellite never travels into full nighttime darkness or full local noon daylight. Figure 10 shows how small the variations are, but in this particular case the high frequency variations are of relatively small magnitude still. The effects on orbit propagation are very small as can be seen in the lower plot of Figure 10.

GRACE

Normal Day. Figure 11 shows the densities and orbit errors for a normal day for GRACE. Notice that GRACE is at a higher altitude than CHAMP for most of its mission life and the densities are about an order of magnitude lower. Consequently, the orbit errors caused by density errors are also considerably lower for GRACE than for CHAMP. The maximum orbit propagation errors here are all less than 10 m. However, the reader should remember that these are errors for densities that have been normalized to the same mean. The Jacchia 71 model would clearly have higher errors without the normalization because of the bias between the Jacchia 71 densities and the other densities that appears in the upper plot of Figure 11.

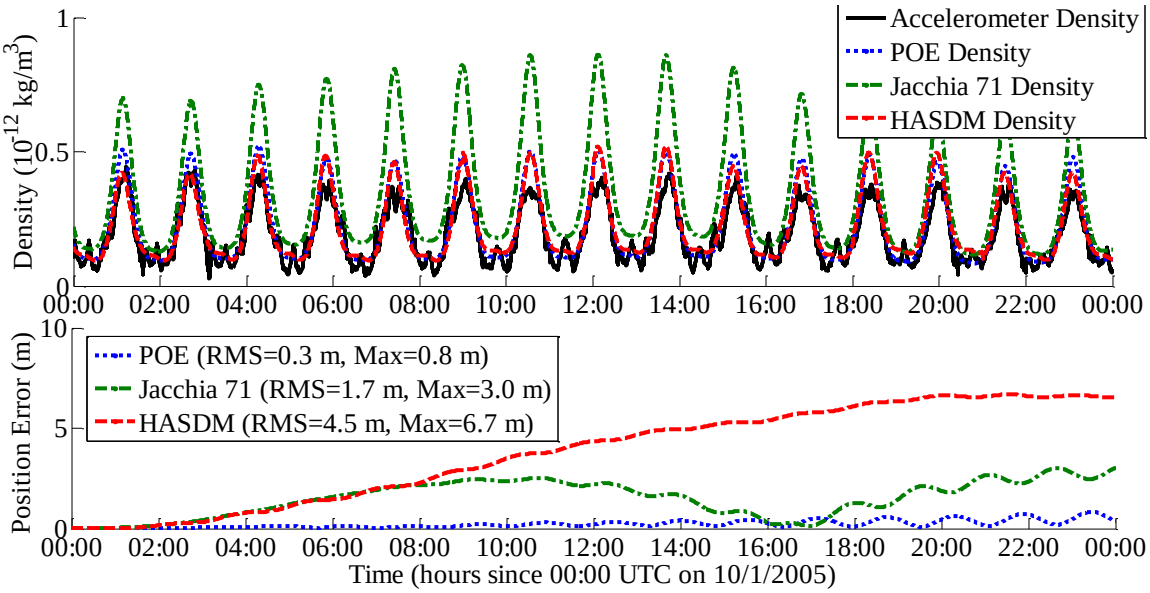

Figure 11. Density and orbit propagation errors along the GRACE orbit on a normal day (October 1, 2005).

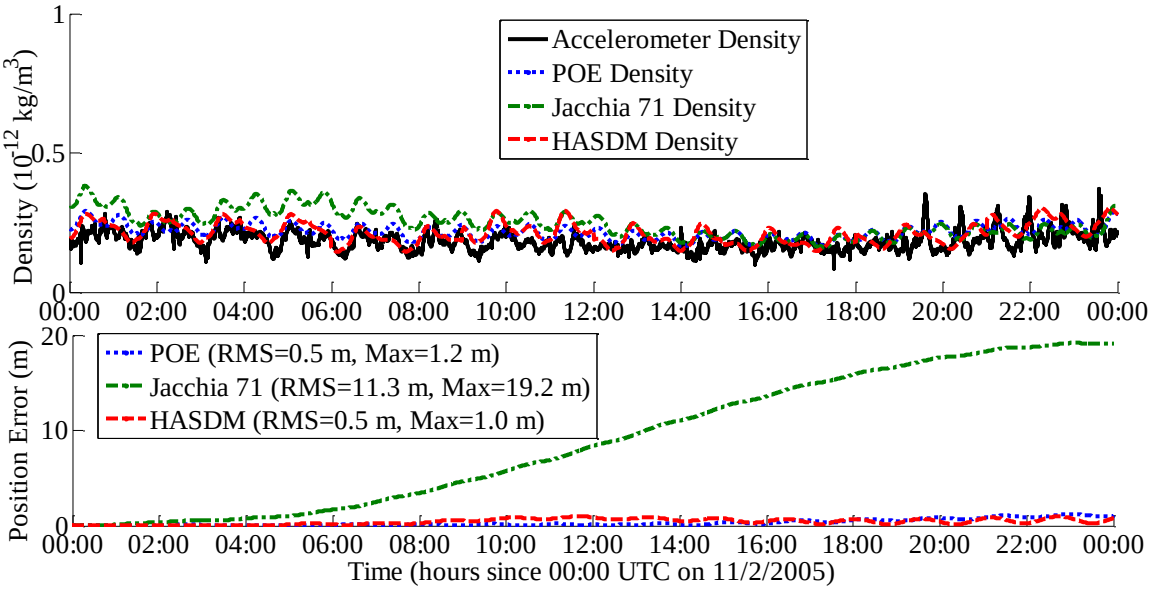

Figure 12. Density and orbit propagation errors along the CHAMP orbit on a day when the CHAMP orbit plane is near terminator (November 2, 2005).

Orbit Plane near the Terminator. The effects of flying near the terminator are more readily seen in GRACE results than in those for CHAMP as seen in Figure 12. The daylight/darkness variations are all very small and the high frequency signals in the accelerometer data are much more apparent than for CHAMP. However, the effects of these unmodeled high frequency variations on the orbit propagation remain quite small with errors for HASDM and POE densities barely exceeding 1 m.

5 Satellite Drag Coefficients and Ballistic Coefficients

5.1 Methodology

The Direct Simulation Monte Carlo (DSMC) method is a computational technique for the simulation of dilute gas flows at the molecular level and is, to date, the basic numerical method in the kinetic theory of gases and rarefied gas dynamics. The DSMC method uses a cell and particle approach to track representative molecules, while probabilistically selecting candidates for intermolecular collisions. Every simulated molecule represents W molecules of real gas, where W is the statistical weight of a simulated molecule. W typically lies in the range of 10^{12} to 10^{25} real molecules per simulated molecule.

The computational domain is divided into mean free path sized cells and molecules in each cell are tracked independently. The positions, velocities, and internal energies (in the case of polyatomic molecules) of simulated molecules are stored in memory and are modified with time as the molecules are concurrently tracked through representative collisions and boundary interactions within the computational domain. The movement and collisions of molecules are decoupled based on the dilute gas approximation. At each time-step, collision probabilities are calculated and collisions are carried out only between molecules in the same cell. The size of the time-step is comparable to the mean collision time[15].
The satellite or spacecraft geometry is inserted into the flow field as a surface mesh. The mesh format differs from one program to another. Molecules are inserted into the flow field either through initial creation at the first time step, a surface flux from the boundaries, or the reservoir method. In typical DSMC simulations, like the flow over a satellite or a vehicle in the Earth's atmosphere, the computational domain is part of a larger flow environment. The boundaries of the computational domain are therefore often set to be free-stream boundaries where molecules are allowed to leave and enter the computational domain and the number of simulated molecules varies with time.

The Three-Dimensional Visual Program (DS3V) was used to model the interactions of simulated molecules with parameterized surfaces and intermolecular collision dynamics. In spite of the computationally demanding nature of DS3V, it was chosen for two main reasons: (i) it is freely available on the internet (www.gab.com.au), and (ii) it is highly reliable and widely used. The only computational parameter specified by the user is the initial number of megabytes used for storage. The size of the cells used to discretize the computational domain is set as a function of this initial number of megabytes defined by the user. The program sets all other computational variables automatically. However, an optional menu is available should the user choose to define the computational parameters such as cell size and timestep.

DS3V does not allow the user to explicitly specify the total energy accommodation coefficient. The default is complete energy accommodation. A workaround for this limitation of DS3V was initially proposed by Pilinski et al. (2011); however, most of their work was limited to complete accommodation. In order to simulate partial energy accommodation (with diffuse reemission) with DS3V, the temperature of the spacecraft surface is set equal to the kinetic temperature of the reemitted molecules. This forces an assumption of single reflection for individual molecules. This means that once a molecule interacts with the surface of the spacecraft, the molecule is assumed to travel a large distance before colliding with another incoming molecule and loses any chance of re-interacting with the surface. Single reflections are dominant in free molecular flow for simple convex geometries. However, caution needs to be taken when dealing with concave and complex geometries. Pilinski et al. (2011) concluded that the difference in drag coefficients computed for concave satellites using single and multiple reflections is on the order of 1%.

5.2 Model Development

The steps involved in the development of the GRACE drag coefficient model are presented in this section.

Step 1: The detailed geometry and surface properties for surface temperature calculations were obtained from the product specification document developed for GRACE. Equations were used to calculate the worst-case surface temperatures for the day and night cycles to be 340 K and 210 K respectively. The detailed geometry and mesh of the GRACE satellite developed for DSMC computations is shown in Figure 12. A highly detailed mesh with approximately 20,000 elements captures all the features needed for the development of a high fidelity model. The CAD geometry was used to calculate the projection areas at different attitude orientations. The geometry was projected onto a plane perpendicular to the flow and the outline of the projection was used to estimate the areas. Since the attitude of the GRACE satellites is controlled, the attitude bounds were set at -3° and 3° for pitch (Φ) and 0° and 3° for sideslip (β). Symmetry was assumed about the X-Z plane. Areas were estimated at 1° intervals and are given in Table 10. The CAD geometry model and estimated areas were validated using the front and side profile areas provided in the GRACE product specification manual.

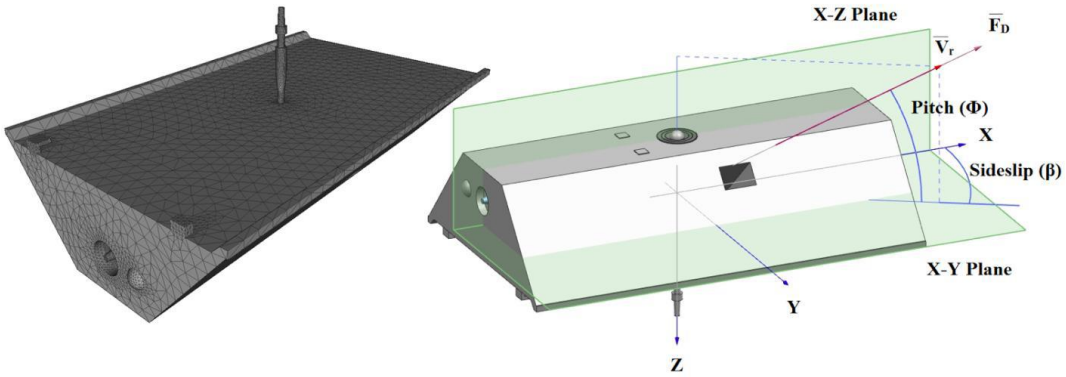

Figure 13: Detailed geometry and mesh with orientation of the GRACE satellite for DSMC computations.

Table 10: GRACE cross-sectional areas as a function of attitude

Φ (right) β (down)	3°	2°	1°	0°	-1°	-2°	-3°
0°	1.311	1.207	1.104	1.004	1.093	1.195	1.299
1°	1.313	1.210	1.113	1.049	1.102	1.198	1.302
2°	1.315	1.224	1.156	1.094	1.145	1.212	1.303
3°	1.335	1.266	1.199	1.139	1.188	1.254	1.323

Step 2: DSMC simulations were performed for all attitude orientations at a large sample of data points along the orbit of GRACE. Days representing different solar and geomagnetic activity levels were carefully chosen for the simulations. Since the mission life of GRACE does not cover elevated or high solar activity days, simulated solar max conditions were used. The atmospheric properties (atmospheric temperature, total number density, and the partial pressures of the atmospheric species constituents) for the DSMC runs were calculated using the NRLMSISE-00 model inbuilt into the Aerospace Toolbox in Matlab®. The semi-empirical energy accommodation coefficient model developed by Pilinski et al. (2010) was used with all its assumptions and limitations. The energy accommodation coefficient model assumed a diffuse gas-surface interaction model.

Step 3: Since DSMC is computationally intensive, C_D cannot be computed real time and a semi-empirical model is needed to estimate C_D at any point in the orbit. A sensitivity analysis was performed on the computed C_D and input parameters for highest correlations to develop the empirical relations. No strong correlations were obtained between the computed total C_D and the input parameters. However, very high correlations were seen between the pressure and shear components of C_D with accommodation coefficient, and free-stream atmospheric temperature respectively, as given in Table 11. Based on the sensitivity profiles of C_D with the different input parameter obtained in Ref 20, power relations were used for the empirical fits.

Table 11: Correlation coefficients of pressure and shear contributions with various input parameters.

	T_∞	V_{rel}	X_{He}	X_O	α
Total	0.400	-0.703	-0.067	-0.518	-0.361
Pressure	-0.667	-0.174	0.698	0.307	-0.997
Shear	0.963	-0.367	-0.737	-0.699	0.705

Step 4: The developed model relations were validated using additional DSMC simulations that were performed at random points in time along the orbit of GRACE. The error in C_D estimated at the random points using the model relations and computed using DSMC was on the order of 1% with a mean of 0.8%.

5.3 Energy Accommodation Coefficient Models

The semi-empirical energy accommodation coefficient (ECAM) model developed by Pilinski et al. (2010) was used for the development of the GRACE C_D model. The limitation of the energy accommodation model used is that the model is not bounded at the lower end by the energy accommodation coefficient of the substrate, α_s (clean surface with no adsorption of atomic oxygen to the surface), originally derived by Goodman (1966). The fraction of the surface covered by adsorbed atomic oxygen becomes smaller as the partial pressure of atomic oxygen decreases. Energy accommodation coefficient of a substrate material, α_s, derived in Goodman (1966) is given as

$$\alpha_s = \frac{K_s \cdot \mu}{(1+\mu)^2}$$

K_s is the substrate coefficient, and μ is the mass ratio of the incoming molecule to the molecules that compose the surface lattice. For a flat plate normal to the flow, K_s is 2.4 when the distribution of the direction of the incoming molecules is random (low speed ratio) and 3.6 for normal incoming flow (high speed ratio). The distribution of the incoming molecules is also a function of the surface geometry. A sphere has a distribution of incoming molecules that is random, even at high speed ratios. GRACE has a geometry that allows normal incidence at high speed ratios. Since the attitude of GRACE is controlled and the computed speed ratios lie in the range of 6 to 11 (relatively high), a value of 3.6 for K_s is more suitable for calculating the accommodation coefficient of the substrate for GRACE.

Modified Semi-Empirical Energy Accommodation Coefficient Model

The modified semi-empirical energy accommodation coefficient model (EACM (MOD)) is a modified version of the original model with Goodman's substrate accommodation implemented. The implementation of Goodman's formula is achieved in a very simple manner. The energy accommodation coefficient in the original model is given as

$$\alpha = \frac{K \cdot n_O \cdot T_\infty}{1 + K \cdot n_O \cdot T_\infty}$$

Where K is the Langmuir fitting parameter and n_O is the number density of atomic oxygen. The energy accommodation coefficient with Goodman's formula implemented is given as

$$\alpha = \frac{\alpha_s + K \cdot n_O \cdot T_\infty}{1 + K \cdot n_O \cdot T_\infty}$$

Semi-Empirical Satellite Accommodation Model

The Semi-Empirical Satellite Accommodation Model (SESAM) is a version of the original energy accommodation coefficient model modified by Pilinski et al. (2010). The modification is the implementation of Goodman's formula to the original model, ECAM. Energy accommodation coefficients as given by SESAM is

$$\alpha = (1-\theta)\alpha_s + \theta\alpha_{ads}$$

Where θ is the effective fractional coverage of atomic oxygen, α_{ads} is the accommodation coefficient of the adsorbate (atomic oxygen), typically assumed to be unity for complete accommodation, and α_s is calculated with K_s of 2.4. θ is calculated in a similar manner to α in the original model ECAM, except for a few minor changes which are not discussed here.

The modified semi-empirical satellite accommodation model (SESAM (MOD)) is essentially the same model as SESAM with 3.6 as the value for K_s in Goodman's[29] formula.

5.4 Results

The developed drag coefficient model for GRACE was used to compute C_D for the duration of the selected days. Comparison of C_D computed using the different energy accommodation coefficient models and constant energy accommodation coefficient of 0.93 (used by Sutton) is performed. Precision attitude and orbit data was provided by Sutton. C_D for attitudes that are within the bounds used in model development is computed using linear interpolation. C_D for attitudes that are beyond the bounds used in model development is computed using linear extrapolation. Precise orbit data was used to obtain atmospheric properties (Tinf and alpha) from NRLMSISE00.

Figure 14 shows the *CD* computed for GRACE using the developed model for July 19, 2005 and simulated solar max conditions. Simulation of solar max conditions uses a 10.7 cm so-lar radio flux index (F10.7) value of 260 and a geomagnetic disturbance index (Ap) value of 21. The percent bias in *CD* computed with a constant energy accommodation coefficient value of 0.93 lie in the range of -7% to 5% with the mean close to 0%. The percent bias in *CD* computed using EACM (MOD) lie in the range of -8% to 3% with the mean close to 0%. The percent bias in *CD* computed SESAM lie in the range of -4% to 7% with the mean close to 2%. The percent bias in *CD* computed SESAM (MOD) lie in the range of -7% to 5% with the mean close to 0%. Since, the constant value of 0.93 for energy accommodation coefficient simulates solar max conditions, the mean different between *CD* computed by Sutton and DSMC using different energy accommodation coefficient models is around 0%. The range and mean of the percent bias between *CD* and density computed using different models and Sutton will henceforth be denoted as (range, mean). The ECAM (MOD) and SESAM (MOD) show identical results because they use the same Goodman's formula with different formulations. The mean bias in *CD* computed using the SESAM model is higher than the other models because it uses 2.4 for Ks in Goodman's formula.

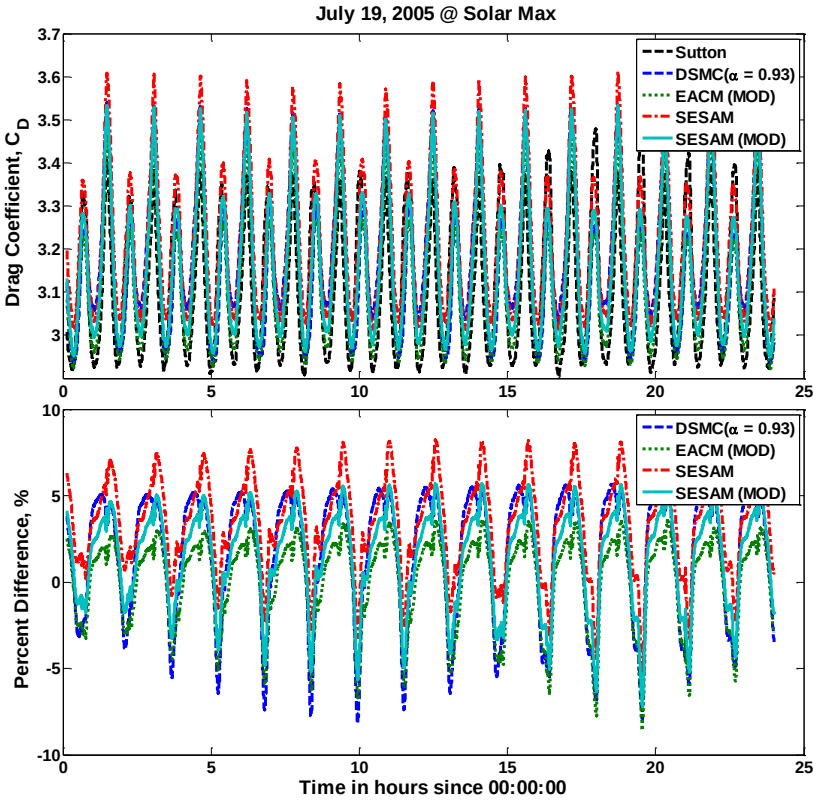

Figure 14: (top) C_D computed using different energy accommodation coefficient models for July 19, 2005 and simulated solar max conditions. (bottom) Percent different in C_D computed using different energy accommodation coefficients model and C_D computed by Sutton's using a flat plate model.

Figure 15**Figure** shows the *CD* computed for GRACE using the developed model for July 19, 2005 and simulated solar min conditions. Simulation of solar min conditions uses a F10.7 value of 50 and an Ap value of 2. The percent bias in *CD* computed with a constant energy accommodation coefficient value of 0.93 lie in the range of -18% to -5% with the mean close to -10%. The percent bias in *CD* computed using EACM (MOD) lie in the range of 3% to 17% with the mean close to 12%. The percent bias in *CD* computed SESAM lie in the range of 7% to 19% with the mean close to 15%. The percent bias in *CD* computed SESAM (MOD) lie in the range of 3% to 17% with the mean close to 12%. The ECAM (MOD) and SESAM (MOD) again show identical results with the mean bias in *CD* computed using the SESAM and Sutton again being higher.

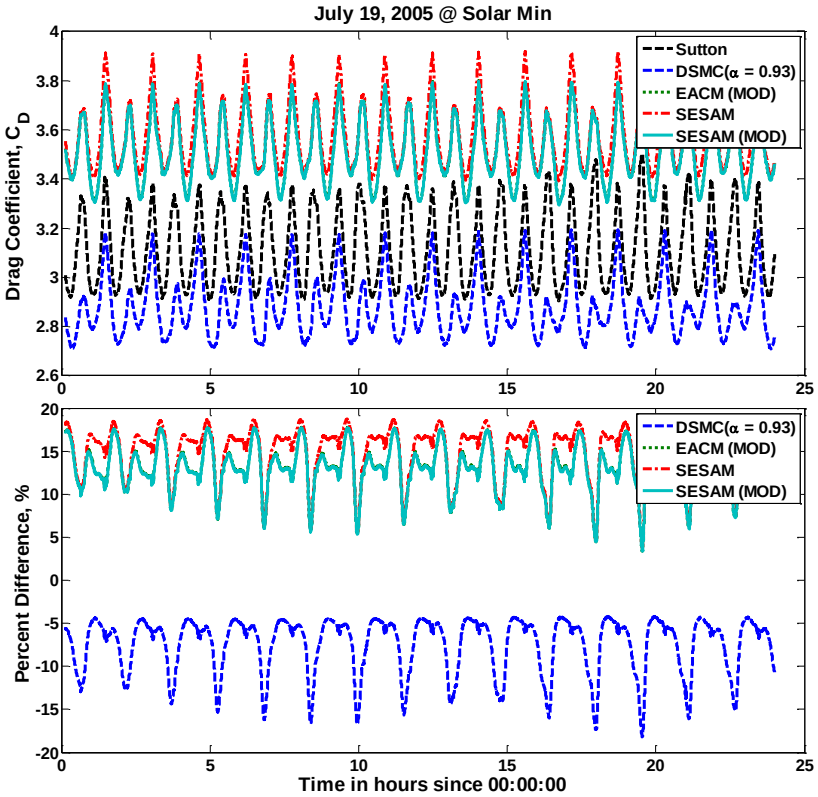

Figure 15: (top) C_D computed using different energy accommodation coefficient models for July 19, 2005 and simulated solar min conditions. (bottom) Percent different in C_D computed using different energy accommodation coefficients model and C_D computed by Sutton's using a flat plate model.

Figure 16 shows the density computed for GRACE by scaling accelerometer-derived densities from Sutton using appropriate *CD* and area ratios for July 19, 2005 and simulated solar min conditions. The percent bias in density computed with a constant energy accommodation coefficient value of 0.93 lie in the range of 2% to 15% with the mean close to 5%. The percent bias in density computed using EACM (MOD) lie in the range of -18% to -8% with the mean close to -15%. The percent bias in density computed SESAM lie in the range of -11% to 2% with the mean close to -6%. The percent bias in density computed SESAM (MOD) lie in the range of -18% to -11% with the mean close to -16%.

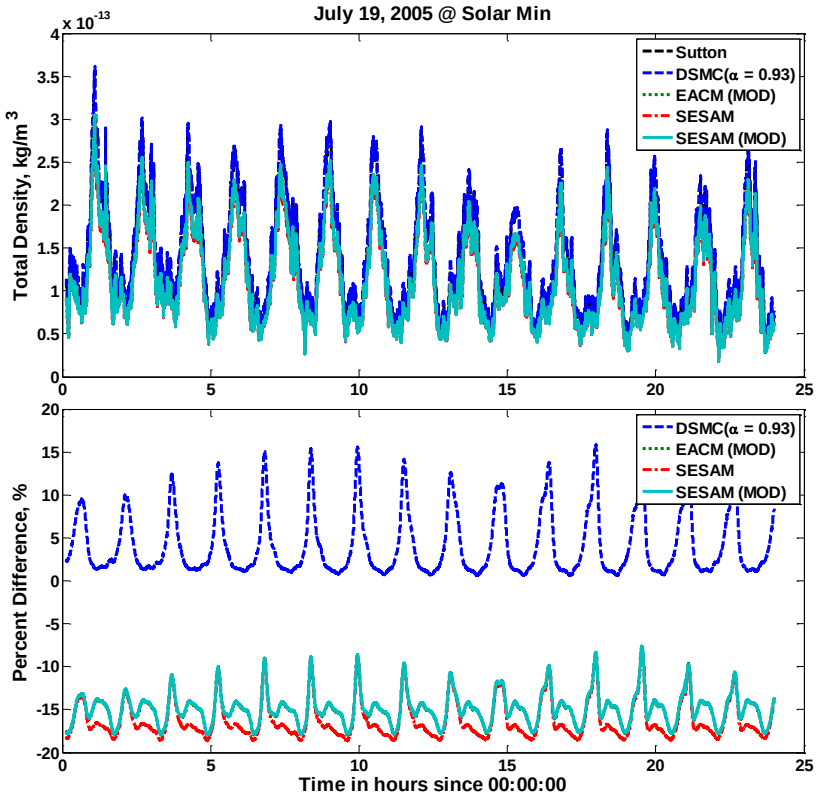

Figure 16: (top) Sutton's accelerometer-derived densities scaled with appropriate C_D and area ratios using different energy accommodation coefficient models for July 19, 2005 and simulated solar min conditions. (bottom) Percent different in density calculated using different energy accommodation coefficients models and accelerometer-derived densities by Sutton.

5 Conclusions

Precision orbit ephemeris (POE) data are used as measurements in an orbit determination process to estimate neutral atmospheric density along the CHAMP and GRACE orbits. The combination of a CIRA 1972 as a baseline density model with ballistic coefficient half-life of 1.8 minutes and density half-life of 180 minutes was found to be the overall combination for estimating POE derived densities that best matched accelerometer derived densities as measured by cross correlation and RMS.

POE derived densities were found for the entire life of CHAMP and from launch through 2011 for GRACE. The density data exists as a continuous data set divided into one week files for ease of access. The POE derived densities were shown to better match, in terms of cross correlation and RMS, the accelerometer derived densities than the HASDM, NRLMSISE-00, and Jacchia 71 density models. The cross correlation between other density sources and the accelerometer derived densities was lower when the orbit plane of the satellite was near the terminator because the high frequency variations observed only by the accelerometer become similar in magnitude to the daylight/darkness variations during an orbit.

Several times during the lifetime of CHAMP and GRACE the satellites' orbits were nearly coplanar. One of those time periods occurred during April 2005. For a few hours during April 3 and again on April 5, the GRACE satellites were flying nearly directly above CHAMP. A comparison was made of the density estimated from CHAMP and GRACE-A during these two days using accelerometer, POE density, HASDM, and the Jacchia 1971 and NRLMSISE-00 models. NRLMSISE-00 and Jacchia 1971

overestimated the densities for both CHAMP and GRACE during these time periods. The POE and HASDM densities matched the overall changes of the accelerometer quite well for CHAMP, but overestimated the sunlit density peaks for GRACE. Also, there are high frequency variations that are only observed by the accelerometers. An interesting feature observed in the accelerometer densities is nocturnal density peaks that occur during both days that correspond to the Midnight Density Maximum phenomena. These peaks are either smoothed through or show up as slight humps or increases in density trough magnitudes for the POE and HASDM densities, but are modeled by NRLMSISE-00.

Densities were estimated for CHAMP, GRACE, and TerraSAR-X for September 26-27, 2007 and September 29-30, 2007. The POE densities were able to accurately observe the major changes seen in the CHAMP and GRACE accelerometers, but not the high frequency variations. Jacchia 1971 significantly overestimated the CHAMP and GRACE densities during these time periods. For TerraSAR-X, at a higher altitude, the POE and Jacchia 1971 densities were very close. This is either because Jacchia 1971 better models the density at higher altitude than at lower altitude or because the density variations are less observable using the POE density technique because of the significantly lower density magnitudes. The strong MDM seen in the CHAMP and GRACE accelerometer densities on April 3 and April 5 of 2005 were observable in the September 26-27 and September 29-30 of 2007 CHAMP accelerometer densities as well. However, they are not observed in the GRACE accelerometer data or in any of the POE densities for CHAMP, GRACE, or TerraSAR-X.

The effects of limited data and lower quality data on density estimation are examined to see the suitability of using a larger set of satellites to estimate density. Discontinuous data sets are created by decimating the original POE data for CHAMP and GRACE. Sets were created with 15 and 8 minutes of data per orbit. Noise levels from 10 cm to 100 m were added to the data to simulate data of lower accuracy. The results showed decreases in cross correlation and RMS of the resulting density estimations compared to accelerometer derived densities. However, the data even for relatively high noise levels should be usable for estimating density. This means many more potential satellites can be used to estimate density providing much better spatial coverage of the thermosphere.

The effects of high frequency variations in atmospheric density on orbit propagation have been examined. The high frequency variations are observed in densities derived from the accelerometers onboard the CHAMP and GRACE satellites, but are not observed in densities derived from precision orbit ephemeris (POE) data, or the Jacchia 71 or HASDM density models. Specific high frequency variations examined were from Traveling Atmospheric Disturbances, polar cusp density enhancements, and the times when the orbit plane was near terminator and high frequency variations are of the same order as daylight/darkness variations. The POE derived densities were superior for orbit propagation compared to Jacchia 71 in all cases and superior or comparable to HASDM in all cases. The errors between the orbits propagated with POE derived densities compared to orbits propagated with accelerometer derived densities were around 1 m for GRACE and ranged from 4-22 m for CHAMP. These errors are not significant for most orbit applications. Therefore, the high frequency variations observed only by the accelerometer are not significant for most orbit analysis applications.

A model to accurately predict the drag coefficient along the orbit of the GRACE satellite was successfully developed using the Direct Simulation Monte Carlo technique. The effect and importance of accurate geometry modeling on drag coefficient has been examined using the developed model. Drag coefficients computed with the model using different energy accommodation coefficients models are compared with those derived by Sutton using a flat plate model and a constant energy accommodation coefficient of 0.93. Drag coefficients computed with the model using a constant accommodation coefficient compared with Sutton show a mean bias in the range of 3-5% with time varying biases going as high as 15% resulting from inaccurate modeling of the geometry. Drag coefficients computed with the model using different energy accommodation co-efficient models show a mean bias in the range of 5-10% with time varying

biases going as high as 19%. Use of a constant energy accommodation coefficient and a flat plate model results in drag coefficients that are consistently and significantly under predicted during solar minimum conditions. During solar maximum conditions, the mean bias in drag coefficients computed with the model and by Sutton is very close to zero; however, time varying biases still reach as high as 6-7%.

The effect of biases in drag coefficient on density estimation using accelerometer data has also been examined. Accurate density estimates have been calculated by scaling the accelerometer-derived densities from Sutton using appropriate drag coefficient and area ratios and different energy accommodation coefficients models. Densities calculated with the model using a constant accommodation coefficient compared with Sutton show a mean bias in the range of 2-3% with time varying biases going as high as 12% resulting from inaccurate modeling of the geometry. Densities calculated with the model using different energy accommodation coefficient models show a mean bias in the range of 8-12% with time varying biases going as high as 18%. Use of a constant energy accommodation coefficient and a flat plate model results in drag coefficients that are consistently and significantly over predicted during solar minimum conditions. During solar maximum conditions, the mean bias in densities calculated with the model and by Sutton is in the range of 4-6% with time varying biases still reaching as high as 11%.

References

Akmaev, R. A., Wu, F., Fuller-Rowell, T. J., Wang, H., Iredell, M. D., "Midnight Density and Temperature Maxima, and Thermospheric Dynamics in Whole Atmosphere Model Simulations," Journal of Geophysical Research, Vol. 115, A08326, doi:10.1029/2010JA015651, 2010.

Anderson, R. L., Born., G. H., and Forbes J. M., "Sensitivity of Orbit Predictions to Density Variability." Journal of Spacecraft and Rockets, Vol. 46, No. 6, 2009, pp. 1214-1230.

Arduini, C., Leneve, G., Herrero, F. A., "Local time and Altitude Variation of Equatorial Thermosphere Midnight Density Maximum (MDM): San Marco Drag Balance Measurements," Geophysical Research, Vol. 24, No. 4, 1997.

Arudra, A. K. "Atmospheric Density Estimation Using Satellite Precision Orbit Ephemerides," M. S. Thesis, Department of Aerospace Engineering, University of Kansas, 2011.

Bowman, B. R., Marcos, F. A., Moe, K., Moe, M. M., "Determination of drag coefficient values for CHAMP and GRACE satellites using orbit drag analysis," Advances in the Astronautical Sciences, 129, 147-166, AAS 07-259, 2008.

Bowman, B., "The Semiannual Thermospheric Density Variation from 1970 to 2002 Between 200-1100 km," Advances in the Astronautical Sciences, 119, 1135-1154, AAS 04-174, 2004.

Bowman, B., F. A. Marcos, and M. J. Kendra, "A method for computing accurate atmospheric density values from satellite drag data," Advances in the Astronautical Sciences, 119, 1117-1134, AAS 04-173, 2004.

Bruinsma S. L., Forbes, J. M., "Storm-time equatorial density enhancements observed by CHAMP and GRACE," Journal of Spacecraft and Rockets, 44, (6), 1154-1159, 2007.

Bruinsma, S., Biancale, R., "Total densities derived from accelerometer data," Journal of Spacecraft and Rockets, 40 (2), No. 2, 230-236, 2003a.

Bruinsma, S., Biancale, R., "Total density retrieval with STAR," First CHAMP Mission Results for Gravity, Magnetic and Atmospheric Studies, Ed. Reigber, C., Luhr, H., Schwintzer, P., Springer, Berlin, 192-199, 2003b.

Bruinsma, S., Forbes, J. M., Nerem, R. S., Zhang, X., "Thermospheric density response to the 20-21 November 2003 solar and geomagnetic storm from CHAMP and GRACE accelerometer data," Journal of Geophysical Research, 111 (AO6303), 1-14, 2006.

Bruinsma, S., Tamagnan, S. D., Biancale, R., "Atmospheric densities derived from CHAMP/STAR accelerometer observations," Planetary and Space Science, 52, 297-312, 2004.

Cefola, P. J., Proulx, R. J., Nazarenko, A. I., Yurasov, V. S., "Atmospheric density correction using two line element sets as the observation data," Advances in the Astronautical Sciences, 116, 1953-1978, AAS 03-626, 2003.

COSPAR Working Group IV, COSPAR International Reference Atmosphere, Akademie-Verlag, Berlin, 1972.

Doornbos, E., Klinkrad, H., Visser, P., "Atmospheric Density Calibration Using Satellite Drag Observations," Advances in Space Research, 36, 515-521, 2005.

Fattig, E., "Comparison of precision orbit derived density estimates for CHAMP and GRACE satellites," M. S. Thesis, Department of Aerospace Engineering, University of Kansas, 2011.

Fattig, E., McLaughlin, C. A., Lechtenberg, T. "Comparison of density estimation for CHAMP and GRACE satellites," *AIAA/AAS Astrodynamics Specialist Conference*, Toronto, ON, AIAA 2010-7976, 2-5 August 2010.

Forbes, J. M., Lu, G., Bruinsma, S., Nerem, S., Zhang, X., "Thermospheric density variations due to the 15-24 April 2002 Solar Events from CHAMP/STAR accelerometer measurements," Journal of Geophysical Research, 110, 1-9, 2005.

Goodman, F. O., and Wachman, H. Y., "Formula for Thermal Accommodation Coefficients," Journal of Chemical Physics, Vol. 46, No. 5, pp. 2376-2386, 1966. doi: 10.1063/1.1841046.

Hedin, A. E., "Extension of the MSIS thermosphere model into the middle and lower atmosphere," Journal of Geophysical Research, 96, 1159-1172, 1991.

Hiatt, A., "Deriving atmospheric density estimates using satellite precision orbit ephemerides," M. S. Thesis, Department of Aerospace Engineering, University of Kansas, 2009.

Hiatt, A., McLaughlin, C. A., Lechtenberg, T., "Deriving density estimates using CHAMP precision orbit data for periods of high solar activity," Advances in the Astronautical Sciences, 134, 23-42, AAS 09-104, 2009.

Jacchia, L. G., Revised Static Models for the Thermosphere and Exosphere with Empirical Temperature Profiles, SAO Special Report No. 332, Smithsonian Institution Astrophysical Observatory, Cambridge, MA, 1971.

Kim, J., "Bridging methods for the JB2006 and NRLMSISE-00 thermospheric density models in the altitude range of 140 km through 200 km," M. S. Thesis, Department of Aerospace Engineering, Pennsylvania State University, August, 2008.

Kim, J., Spencer, D. B., Kane, T. J., Urbina, J., "A blending technique in thermospheric density modeling," AIAA/AAS Astrodynamics Specialist Conference and Exhibit, AIAA, Honolulu, Hawaii, 18-19 August, 2008.

Kim, J., Spencer, D. B., Kane, T. J., Urbina, J., "Thermospheric density model blending techniques: Bridging the gap between satellites and sounding rockets," Radio Science, 44 (RSO 22), 2009.

Konig, R. Neumayer, K. H., "Thermospheric events in CHAMP precise orbit determination," First CHAMP Mission Results for Gravity, Magnetic and Atmospheric Studies, Ed. Reigber, C., H. Luhr, H., Schwintzer, P., Springer, Berlin,112-119, 2003.

Konig, R., Michalak, G., K. Neumayer, K. H., Zhu, S., "Remarks on CHAMP orbit products," Observation of the Earth System from Space, Ed. Flury, J., Rummel, R., Reigber,C., Rothacher, M., Boedecker, G., Schreiber, U., Springer, Berlin, 17-26, 2006.

Konig, R., Michalak, G., Neumayer, K. H., Zhu, S. Y., Meixner, H.,Reigber, C., "Recent developments in CHAMP orbit determination at GFZ," Earth Observation with CHAMP Results from Three Years in Orbit, Ed. Reigber, C., Luhr, H., Schwintzer, P., Wickert, J., Springer, Berlin, 65-70, 2005.

Konig, R., Zhu, S., Reigber, C., Neumayer, K. H., Meixner, H., Galas, R., Baustert, G., "CHAMP rapid orbit determination for GPS atmospheric limb sounding," Advances in Space Research, 30 (2), 289-293, 2002.

Lechtenberg, T., "Derivation and observability of upper atmospheric density variations utilizing precision orbit ephemerides," M. S. Thesis, Department of Aerospace Engineering, University of Kansas, 2010.

Lechtenberg, T. F., C. A. McLaughlin, T. Locke, and D. Mysore Krishna, "Thermospheric Density Variations: Observability using Precision Satellite Orbits and Effects on Orbit Propagation," *Space Weather*, Vol. 11, pp. 34-45, doi:10.1029/2012SW000848.

Locke, T., "Further Developments in Orbit Ephemeris Derived Neutral Density," M. S. Thesis, Department of Aerospace Engineering, University of Kansas, 2012.

Mance, S. R., "An Investigation into Satellite Drag Modeling Performance," M. S. Thesis, Department of Aerospace Engineering, University of Kansas, 2010.

Marcos, F. O., Wise, J. O., Kendra, M. J. Grossbard, N. J., "Satellite drag research: past, present, and future," Advances in the Astronautical Sciences, 116, 1865-1878, AAS 03-620, 2003.

McLaughlin, C. A., "Upper atmospheric phenomena and satellite drag," Advances in the Astronautical Sciences, 123, 989-996, AAS 05-315, 2005.

McLaughlin, C. A., Bieber, B. S., "Neutral density determined from CHAMP precision orbits," Advances in the Astronautical Sciences, 129, 167-186, AAS 07-260, 2007.

McLaughlin, C. A., Fattig, E., Mysore Krishna, D., Locke, T., Mehta, P. M., "Time Periods of Anomalous Density for CHAMP and GRACE," Advances in the Astronautical Sciences, 142, 3299-3310, AAS 11-613, 2011a.

McLaughlin, C. A., Hiatt, A., Bieber, B. S., "Comparison of total density derived from CHAMP precision orbits and CHAMP accelerometer," Advances in the Astronautical Sciences, 130, 1193-1206, AAS 08-177, 2008a.

McLaughlin, C. A., Hiatt, A., Fattig, E., Lechtenberg, T., "Ballistic coefficient and density estimation," Advances in the Astronautical Sciences, 135, 2269-2285, AAS 09-439, 2009.

McLaughlin, C. A., Hiatt, A., Lechtenberg, T., "Calibrating precision orbit derived total density," AIAA/AAS Astrodynamics Specialist Conference, Honolulu, HI, AIAA 2008-6951, 18-21 August 2008b.

McLaughlin, C. A., Hiatt, A., Lechtenberg, T., "Precision orbit derived total density," Journal of Spacecraft and Rockets, 48 (1), 166-174, 2011b.

McLaughlin, C. A., Lechtenberg, T., Fattig, E., Mysore Krishna, D., "Estimating density using precision satellite orbits from multiple satellites," Journal of the Astronautical Sciences, 2013 (in press).

McLaughlin, C. A., T. Locke, and D. Mysore Krishna, "Effects of High Frequency Density Variations on Orbit Propagation," Space Flight Mechanics 2012, Vol. 143 of Advances in the Astronautical Sciences, 2012, AAS 12-176, pp. 1061-1068.

McLaughlin, C. A., S. Mance, and T. Lechtenberg, "Drag Coefficient Estimation in Orbit Determination," Journal of the Astronautical Sciences, Vol. 58, No. 3, Part 2, 2011, pp. 513-530.

Mehta, P. M., McLaughlin, C. A., "Density and ballistic coefficient estimation revisited," Advances in the Astronautical Sciences, 142, 3247-3264, AAS 11-609, 2011.

Mehta, P. M., McLaughlin, C. A., "GRACE Drag Coefficient Model Developed using Direct Simulation Monte Carlo (DSMC) Method," Space Flight Mechanics 2013, Vol. 148 of Advances in the Astronautical Sciences, 2013, AAS 13-284, pp. 1281-1298.

Mehta, P. M., C. A. McLaughlin, T. F. Lechtenberg, and S. Mance, "Energy-Accommodation Coefficient and Drag Coefficient Modeling for Stella and Starlette, 63rd International Astronautical Conference, Naples, Italy, October 1-5, 2012.

Michalak, G., Baustert, G., Konig, R., Reigber, C., "CHAMP rapid science orbit determination: status and future prospects," First CHAMP Mission Results for Gravity, Magnetic and Atmospheric Studies, Ed. Reigber, C., Luhr, H., Schwintzer, P., Springer, Berlin, 98-103, 2003.

Montenbruck, O., van Helleputte, T., Kroes, R., Gill, E., "Reduced dynamic orbit determination using GPS code and carrier measurements," Aerospace Science and Technology, 9, 261-271, 2005.

Mysore Krishna, D., "Improving and expanding precision orbit derived atmospheric densities" M. S. Thesis, Department of Aerospace Engineering, University of Kansas, 2012.

Mysore Krishna, D., McLaughlin, C. A., "Combining precision orbit derived density estimates," *Advances in the Astronautical Sciences*, 142, 3229-3246, AAS 11-475, 2011.

Nerem, R. S., Forbes, J. M., Sutton, E. K., Bruinsma, S., "Atmospheric density measurements derived from CHAMP/STAR accelerometer data," Advances in the Astronautical Sciences, 116, 1879-1898, AAS 03-621, 2003.

Nerem, R. S., Lerch, F. J., Marshall, J. A., Pavlis, E. C., Putney, B. H., Tapley, B. D., Eanses, R. J., Ries, J. C., Schutz, B. E., Shum, C. K., Watkins, M. M., Klosko, S. M., Chan, J. C., Luthcke, S. B., Patel, G. B., Pavlis, N. K., Williamson, R. G., Rapp, R. H., Biancale, R., Nouel, F., "Gravity model developments for Topex/Poseidon: Joint Gravity Models 1 and 2," Journal of Geophysical Research, 99 (C12), p. 24421-24447, 1994.

Picone, J. M., Hedin, A. E., Drob, D. P., "NRLMSISE-00 empirical model of the atmosphere: statistical comparisons and scientific issues," Journal of Geophysical Research, 107 (A12), 2002.

Pilinski, M., Argrow, B., and Palo, S., **"**Drag Coefficients of Satellites with Concave Geometries: Comparing Models and Observations**,"** Journal of Spacecraft and Rockets, Vol. 48, No. 2, March-April 2011, pp. 312-325.

Pilinski, M., Argrow, B., and Palo, S., "Semi-Empirical Model for Satellite Energy Accommodation Coefficients," Journal of Spacecraft and Rockets, Vol. 47, No. 6, November-December 2010, pp. 951-956.

Rhoden, E. A., Forbes, J. M., Marcos, F. A., "The influence of geomagnetic and solar variability on lower thermospheric density," Journal of Atmospheric and Solar-Terrestrial Physics, 62, 999-1013, 2000.

Roberts, C. E., Jr., "An analytic model for upper atmosphere densities based upon Jacchia's 1970 models," Celestial Mechanics, 4 (3-4), 368-377, 1971.

Sabol, C., Luu, K. K., "Atmospheric density dynamics and the motion of satellites," AMOS Technical Conference, Wailea, HI, September 2002.

Schaeperkoetter, A., C. McLaughlin, "Effects of Density Variations in the Upper Atmosphere on Satellite Trajectories," Space Flight Mechanics 2010, Vol. 136 of Advances in the Astronautical Sciences, 2010, AAS 10-223, pp. 1817-1830.

Schlegel, K., Luhr, H., St. Maurice, J. P., Crowley, G., Hackert, C., "Thermospheric density structures over the polar regions observed with CHAMP," Annales Geophysicae, 23, 1659-1672, 2005.

Storz, M. F., Bowman, B. R., Branson, J. I., Casali, S. J., Tobiska, W. K.., "High Accuracy Satellite Drag Model (HASDM)," Advances in Space Research, 36 (12), 2497-2505, 2005.

Sutton, E. K., Forbes, J. M., Nerem, R. S., Woods, T. N., "Neutral density response to the solar flares of October and November, 2003," Geophysical Research Letters, 33, 2006.

Sutton, E. K., Nerem, R. S., Forbes, J. M., "Global thermospheric neutral density and wind response to the severe 2003 geomagnetic storms from CHAMP accelerometer data," Journal of Geophysical Research, 110, 2005.

Sutton, E. K., Nerem,R. S., Forbes, J. M., "Density and winds in the thermosphere deduced from accelerometer data," Journal of Spacecraft and Rockets, 44 (6), 1210-1219, 2007.

Tanygin, S., Wright, J. R., "Removal of arbitrary discontinuities in atmospheric density modeling," Advances in the Astronautical Sciences, 119, 1185-1196, AAS 04-176, 2004.

Tapley, B., Ries, J., Bettadpur, S., Chambers, D., Cheng, M., Condi, F., Gunter, B., Kang, Z., Nagel, P., Pastor, R., Pekker, T., Poole, S., Wang, F., "GGM02 - An improved Earth gravity field model from GRACE," Journal of Geodesy, 2005, DOI 10.1007/s00190-005-0480-z

Tapley, B. D., Ries, J. C., Bettadpur, S., Cheng, M., "Neutral Density Measurements for the Gravity Recovery and Climate Experiment Accelerometers," Journal of Spacecraft and Rockets, 44 (6), 1220-1225, 2007.

Vallado, D. A., Fundamentals of Astrodynamics and Applications, Chap. 8, App. B, Microcosm Press, El Segundo, CA, 3rd Edition, 2007.

van den Ijssel, J., Visser, P., "Determination of non-gravitational accelerations from GPS satellite-to-satellite tracking of CHAMP," Advances in Space Research, 36, 418-423, 2005.

van den Ijssel, J., Visser, P., "Performance of GPS accelerometry: CHAMP and GRACE," Advances in Space Research, 39, 1597-1603, 2007.

van den Ijssel, J., Visser, P., Haagmans, R., "Determination of non-gravitational accelerations from orbit analysis," Earth Observation with CHAMP Results from Three Years in Orbit, Ed. Reigber, C., Luhr, H., Schwintzer, P., Wickert, J., Springer, Berlin, 95-100, 2005.

Wilkins, M. P., Sabol, C. A., Cefola, P. J., Alfriend, K. T., "Improving Dynamic Calibration of the Atmosphere," Advances in the Astronautical Sciences, 127, 1257-1272, AAS 07-185, 2007a.

Wilkins, M. P., Sabol, C. A., Cefola, P. J., Alfriend, K. T., "Validation and application of corrections to the NRLMSISE-00 atmospheric density model," Advances in the Astronautical Sciences, 127, 1285-1304, AAS 07-189, 2007b.

Willis, P., Deleflie, F., Barlier, F., Bar-Sever, Y. E., and Romans, L. J., "Effects of thermosphere total density perturbations on LEO orbits during severe geomagnetic conditions (Oct-Nov 2003) using DORIS and SLR data," Advances in Space Research, 36, 522-533, 2005.

Wright, J. R., "Real-Time Estimation of Local Atmospheric Density," Advances in the Astronautical Sciences, 114, 927-950, AAS 03-164, 2003.

Wright, J. R., Woodburn, J., "Simultaneous real-time estimation of atmospheric density and ballistic coefficient," Advances in the Astronautical Sciences, 119, 1155-1184, AAS 04-175, 2004.

Yurasov, V. S., Nazarenko, A. I., Alfriend, K. T., Cefola, P. J., "Reentry time prediction using atmospheric density corrections," Journal of Guidance, Control, and Dynamics, 31 (2), 282-289, 2008.

Yurasov, V. S., Nazarenko, A. I., Cefola, P. J., Alfriend, K. T., "Results and issues of atmospheric density correction," Journal of the Astronautical Sciences, 52 (3), 281-300, 2004.